

## Article

# Effect of Phosphorus, Iron, Zinc, and Their Combined Deficiencies on Photosynthetic Characteristics of Rice (*Oryza sativa* L.) Seedlings

Dapeng Gao <sup>1,†</sup>, Cheng Ran <sup>1,†</sup>, Kun Dang <sup>1,†</sup>, Xiaolei Wang <sup>1</sup>, Yunhe Zhang <sup>1</sup>, Yanqiu Geng <sup>1</sup>, Shuying Liu <sup>2</sup> , Zhengwen Guan <sup>1</sup>, Liying Guo <sup>1,\*</sup> and Xiwen Shao <sup>1,\*</sup>

<sup>1</sup> Agronomy College, Jilin Agricultural University, Changchun 130118, China

<sup>2</sup> College of Life Science, Jilin Agricultural University, Changchun 130118, China

\* Correspondence: guoliying0621@163.com (L.G.); shaoxiwen@126.com (X.S.)

† These authors contributed equally to this work.

**Abstract:** Combined elemental deficiencies are more complex and insidious physiological metabolic responses than single elemental stresses. To determine the effects of phosphorus (P), iron (Fe), zinc (Zn), and their deficient combinations on photosynthetic characteristics of rice seedlings, we investigated their effects on dry weight, chlorophyll (Chl) content, rapid photosynthetic carbon assimilation CO<sub>2</sub> responses, and Chl fluorescence in four-week-old rice (CB9 and BJ1 cultivars) seedlings. The results showed that the dry matter, maximum carboxylation efficiency ( $V_{c,max}$ ), and maximum electron transfer efficiency ( $J_{max}$ ) of seedlings were all reduced to different degrees under the element deficiency treatments. JIP-test analysis showed that the decrease in the concentration of active PSII reaction centers (RC/ABS) under -Zn treatment was the main reason for the inhibition of performance index  $PI_{ABS}$ . The -P treatment reduced RC/ABS and inhibited electron transfer ( $\psi_{Eo}$ ). Primary photochemical reactions ( $\varphi_{Po}$ ) of -P-Zn treated seedlings were also inhibited compared to the -P treatment. The -Fe and -Fe-Zn treatments inhibited photosynthesis most severely, which not only reduced RC/ABS but also severely inhibited  $\varphi_{Po}$  and  $\psi_{Eo}$ . Notably, the -P-Fe and -P-Fe-Zn treatments of the CB9 improved the RC/ABS, alleviating the limitation of Fe deficiency. These results help enhance the understanding of the complex relationship between nutrient balance and photosynthesis, especially for P, Fe, Zn, and their combined deficiency.

**Keywords:** phosphate iron and zinc; rice; photosynthetic characteristic; Chl a fluorescence; JIP-test



**Citation:** Gao, D.; Ran, C.; Dang, K.; Wang, X.; Zhang, Y.; Geng, Y.; Liu, S.; Guan, Z.; Guo, L.; Shao, X. Effect of Phosphorus, Iron, Zinc, and Their Combined Deficiencies on Photosynthetic Characteristics of Rice (*Oryza sativa* L.) Seedlings. *Agronomy* **2023**, *13*, 1657. <https://doi.org/10.3390/agronomy13061657>

Academic Editor: Guanfu Fu

Received: 4 April 2023

Revised: 18 June 2023

Accepted: 18 June 2023

Published: 20 June 2023



**Copyright:** © 2023 by the authors. Licensee MDPI, Basel, Switzerland. This article is an open access article distributed under the terms and conditions of the Creative Commons Attribution (CC BY) license (<https://creativecommons.org/licenses/by/4.0/>).

## 1. Introduction

Rice (*Oryza sativa* L.) is one of the world's most important food crops and contains almost 70% calories, 65% protein, and most of the trace elements required by people [1]. Rice is widely adaptable and grows in acidic and alkaline environments [2,3]. However, nutrient availability to rice is generally imbalanced because of the physicochemical properties of the soil and the tillage system, as well as the interaction between elements [4]. For example, rice is prone to suffer from nutrient deficiencies, such as potassium, phosphorus (P), iron (Fe), zinc (Zn), and calcium deficiencies in saline environments [2,5]. Rice is susceptible to Fe toxicity stress, and increased inter-root Fe may reduce P and K uptake in acidic environments [3,6]. In addition, photosynthesis is the most sensitive process in plant physiological metabolism [7,8], and nutrient deficiencies can directly or indirectly adversely affect photosynthesis. However, improving the understanding of the adverse effects of elemental deficiencies and their combinations on photosynthesis is necessary to ensure sustained rice production.

P is a component of essential biomolecules, such as nucleic acids, energy, phospholipids, and phytic acid [4,9]. P deficiency affects energy transfer in electron transport, reducing the RuBP pool size and the photosynthetic CO<sub>2</sub> assimilation capacity of leaves,

reducing their photosynthetic performance and inhibiting normal plant growth [10,11]. Fe is a micronutrient essential for cellular functions and is widely involved in redox reactions in plants, where it also acts as a cofactor in metabolic pathways [9]. Fe is present in almost all components of the electron transport chain in chloroplasts, and up to 80% of the Fe in leaves is found in chloroplasts [12]. Fe deficiency not only leads to chlorotic phenotype, but also to a reduction in the amount of active photo-oxidizable P700 and the degradation of the photosystem I subunit, which severely inhibits photosynthesis in leaves [12–15]. Zn plays structural and catalytic roles in enzymes involved in various important metabolic and regulatory processes [16,17]. When plants are Zn deficient, chloroplasts become swollen and deformed, the chloroplast matrix zone expands, chlorophyll content decreases, and the activity of photosystem II is inhibited [18]. Zinc deficiency can also cause plants to exhibit symptoms such as reduced leaf size and shortened internodes, leading to crop growth inhibition and reduced yields [17,18]. P, Fe, and Zn play important roles in plants, and their deficiency is universally and substantially damaging to plants. Until now, the lack of multiple element combinations on plant growth and ionic interactions has been poorly understood. Thus, it is important to explore the combined absence of P, Fe, and Zn for plant growth.

Research on nutrients has found special relationships between nutrients; enrichment or deficiency of one or more nutrients may affect the uptake among the utilization of other nutrients by plants [19,20]. Research has revealed interactions between multiple elements and more complex, insidious physiological metabolic responses than those caused by single-nutrient stress [20]. Nitrogen (N) actively controls the phosphate starvation response in plants [21]. Zn can promote the translocation of N to rice leaves and seeds and improve N utilization [17]. Low P can promote Fe uptake, and the combined treatment of low P and low Fe can promote the elongation of the primary roots of rice plants [11,22]. Zinc is antagonistic to many metals such as Fe and cadmium (Cd). For example, high Zn content can reduce the uptake of Fe by plants and has great potential to reduce the toxicity of heavy metals in some plants [9,23,24]. Notably, P and Fe homeostasis has been shown to antagonistically regulate the growth of rice seedlings. Studies have shown that Fe deficiency can severely limit seedling growth in rice, but a combination of Fe and P deficiencies can reverse the Fe limitation [4,9,12]. These studies help in explaining plant growth performance, developing effective fertilizer management strategies, and breeding new varieties. However, these studies have mainly focused on the growth of crops and the interactions between elements and less on the photosynthetic properties of leaves.

In this study, we grew rice seedlings in environments deficient in three elements, P, Fe, and Zn, and their combinations thereof, and explored the effects these deficiencies on the photosynthetic performance of rice leaves by analyzing rapid Chl *a* fluorescence induction kinetics and fast A-Ci response curves to improve the understanding of the interplay between nutrient homeostasis and photosynthesis. Our objectives were as follows: (a) to explore the effects of these deficiencies on rice seedling growth, and (b) to explore the effect of combined deficiencies on the photosynthetic performance of rice leaves. The results are expected to provide new insights into the relationship between phosphorus, iron, zinc, and their combined deficiencies and photosynthetic performance in rice.

## 2. Materials and Methods

### 2.1. Experimental Design

Changbai 9 (cultivars, CB9) and Baijing 1 (cultivars, BJ1) were used as test materials. Uniformly sized seeds were disinfected in a 5% sodium hypochlorite solution for 10 min. Sterilized seeds were germinated in distilled water at 30 °C for 2 d in the dark and then incubated at 30 °C in the light for 2 d. Germinated seeds were selected and placed in 96-well plastic plates. The plates were then placed in plastic boxes (19 cm long, 14 cm wide, and 13 cm high) and incubated in distilled water and 1/2 full strength nutrient solution for 3 days each, transferred to the full nutrient solution of the International Rice Research Institute [25] (containing 1.45 mM NH<sub>4</sub>NO<sub>3</sub>, 0.323 mM NaH<sub>2</sub>PO<sub>4</sub>·2H<sub>2</sub>O,

0.512 mM  $K_2SO_4$ , 0.998 mM  $CaCl_2$ , 1.643 mM  $MgSO_4 \cdot 7H_2O$ , 9.1  $\mu M$   $MnCl_2 \cdot 4H_2O$ , 0.075  $\mu M$   $(NH_4)_6Mo_7O_{24} \cdot 4H_2O$ , 18.882  $\mu M$   $H_3BO_3$ , 0.152  $\mu M$   $ZnSO_4 \cdot 7H_2O$ , 0.155  $\mu M$   $CuSO_4 \cdot 5H_2O$ , 0.036 mM  $FeCl_3 \cdot 6H_2O$ , and 0.031 mM  $Na_2EDTA \cdot 2H_2O$ , 0.071 mM Citric acid monohydrate, and 500 mL of concentrated sulfuric acid were added every 10 L (pH 5.4)) for 3 weeks, and then sampled for determination. Hydroponic experiments were conducted in an artificial climate chamber. It used a 14 h light (28 °C)/10 h dark (22 °C) photoperiod with light intensity of 350  $\mu mol m^{-2} s^{-1}$  and relative humidity maintained at about 70%. When the full nutrient solution treatment was CK for P, Fe, and Zn deficiency and their combined stress treatments (-P-Fe, -P-Zn, -Fe-Zn, -P-Fe-Zn),  $NaH_2PO_4$ ,  $ZnSO_4$ , or Fe-EDTA in the nutrient solution were omitted. The nutrient solution was renewed every 3 d, and the pH was adjusted daily to 5.5–5.6. A total of 96 biological replicates were set up for each treatment.

## 2.2. Sample Determination and Collection

Samples of uniform length and size were selected and used first for the determination of the rapid Chl fluorescence induction kinetic curve ( $n = 20$ , 6 highly representative replicates were randomly selected for statistical analysis) and A-Ci response curves (at least 3 replicates). Plants after measuring chlorophyll fluorescence curves were used for determination of the total chlorophyll content and dry matter weight.

### 2.2.1. Dry Matter Weight (DW)

We selected five young plants of uniform growth, removed the root system, killed them at 105 °C for 30 min, dried them at 80 °C to a constant weight, and weighed them.

### 2.2.2. Total Chl Content (T Chl)

Freshly expanded uppermost leaves (0.2 g) were incubated overnight at room temperature in 15 mL of 80% acetone in the dark, using the method of Nam et al. [12]. The total Chl content of the leaves was measured using a UV-Vis spectrophotometer (UV-2600; Shimadzu, Japan). The absorbance of the supernatant was measured at 645 and 663 nm. The total Chl concentration was calculated using the following equation:

$$\text{Total Chl} = (20.31 \times A_{645} + 8.05 \times A_{663}) / \text{FW} \quad (1)$$

where FW represents fresh weight. As the different treatments resulted in different plant sizes, leaves from more than five seedlings were selected from each replicate for the assay ( $n = 3$ ).

### 2.2.3. Rapid A–Ci Response

Following the method of Stinziano et al. [26], differential gas analysis of  $CO_2$  and  $H_2O$  was performed on the topmost unfolded leaf of each intact plant by using the high-speed  $CO_2$  ramping technique and a portable photosynthesis system (CIRAS-3, PP Systems International, Inc., Amesbury, MA, USA) to obtain A-Ci response curves. The program parameters were set as follows: saturated light intensity, 1200  $\mu mol$  (photons)  $m^{-2} s^{-1}$ ; flow rate, 300  $cc min^{-1}$ ; relative humidity, 60%; and leaf temperature, 30 °C.  $CO_2$  concentration varied from 50 to 1800  $\mu mol mol^{-1}$ . The A-Ci curves were further analyzed using the model (FvCB) proposed by Farquhar et al. [27] to obtain the maximum Rubisco carboxylation rate ( $V_{c,max}$ ) and the maximal electron transport rate ( $J_{max}$ ).

### 2.2.4. Chl a Fluorescence Transient

After 30 min of dark adaptation, the leaves were subjected to a rapid Chl a fluorescence induction kinetic curve (OJIP curve) using M-PEA (Hansatech Instruments Ltd., Norfolk, UK). The OJIP curve was induced by red light at 3000  $\mu mol$  (photons)  $m^{-2} s^{-1}$  for 2 s. Points O, K, J, and I represent the fluorescence intensities corresponding to 20  $\mu s$ , 300  $\mu s$ , 2 ms, and 30 ms, respectively, and point P represents the maximal fluorescence intensity

(generally  $F_P \approx F_M$ ). The OJIP curves were normalized to the O-P, O-J, and O-K points according to the JIP-test analysis.

$$\text{The O-P point was normalized by } V_t = (F_t - F_O)/(F_M - F_O); \quad (2)$$

$$\text{The O-K point was normalized by } W_{OK} = (F_t - F_O)/(F_K - F_O); \quad (3)$$

$$\text{The O-J point was normalized by } W_{OJ} = (F_t - F_O)/(F_J - F_O); \quad (4)$$

$$\text{and the O-I point was normalized by } W_{OI} = (F_t - F_O)/(F_I - F_O). \quad (5)$$

The fluorescence transients were analyzed according to the JIP-test equations [28]. The meanings and calculation formulas of the parameters are listed in Table A1.

### 2.3. Statistical Analyses

Data were analyzed using analysis of variance (ANOVA). One-way ANOVA with Duncan's post hoc test was used separately for each rice genotype to compare means. For all statistical analyses, differences were considered statistically significant for  $p < 0.05$ . All observations were recorded, and the data are expressed as mean  $\pm$  standard deviation (SD) ( $n \geq 3$ ).

## 3. Results

### 3.1. Phenotypes and Dry Weight

As shown in Figure 1, nutrient deficiencies inhibit the growth of rice seedlings to varying degrees, evidenced by reduced plant height, thinner stalks, and/or yellowing of leaves. The dry weight of the CB9 cultivar varied as CK > -Zn > -P-Zn > -P > -P-Fe > -P-Zn-Fe > -Fe  $\geq$  -Zn-Fe, and that of the BJ1 cultivar varied as CK > -Zn > -P-Zn  $\geq$  -P > -P-Zn-Fe  $\geq$  -Zn-Fe  $\geq$  -P-Fe  $\geq$  -Fe. The inhibitory effect of a single-nutrient deficiency on growth was consistent for both rice varieties, with CK > -Zn > -P > -Fe. Compared with CK, the dry weights of the two varieties with -P-Zn and -Fe treatments were significantly reduced by 56.58%, 79.21%, and 95.66% (CB9) and 42.89%, 63.46%, and 94.10% (BJ1), respectively. However, the combination of these three element deficiencies had different effects on the two rice varieties. The CB9 cultivar showed a dry weight reduction in the order -P-Zn > -P-Fe > -P-Zn-Fe > -Zn-Fe, with significant differences between treatments, and the BJ1 cultivar showed a dry weight reduction in the order -P-Zn > -P-Zn-Fe  $\geq$  -Zn-Fe  $\geq$  -P-Fe, with non-significant differences between treatments, except for the -P-Zn treatment. Notably, both varieties showed a trend of -P-Zn  $\geq$  -P and -P-Fe  $\geq$  -Fe in dry weight reduction (CB9 differed significantly with 15.40% and 73.25%, respectively, whereas BJ1 was not significant with 2.07% and 6.69%, respectively).

### 3.2. Total Chl Content

As shown in Figure 2, the total Chl content of the two rice varieties under P, Fe, Zn, and their combined deficiency stress behaved differently, with the CK and -Zn treatments having the highest and the -Fe-Zn and -Fe treatments having the lowest total Chl content. Specifically, among the CB9 cultivar, the CK, P, and Zn treatments had the highest total Chl content and were not significantly different. The other treatments showed total Chl content in the order -P-Zn > -P-Fe > -P-Fe-Zn > -Fe-Zn  $\geq$  -Fe, with decreases of 5.03%, 44.33%, 58.17%, 84.05%, and 84.20%, respectively, compared with CK. By contrast, the BJ1 cultivar with -P treatment had a lower total Chl content than that with the CK and -Zn treatment and was not significantly different from -P-Zn. The other treatments showed total Chl content in the order -P-Zn > -P-Fe-Zn > -P-Fe > -Fe-Zn  $\geq$  -Fe, with decreases of 6.00%, 73.20%, 76.60%, 82.04%, and 82.67%, respectively, compared with CK.

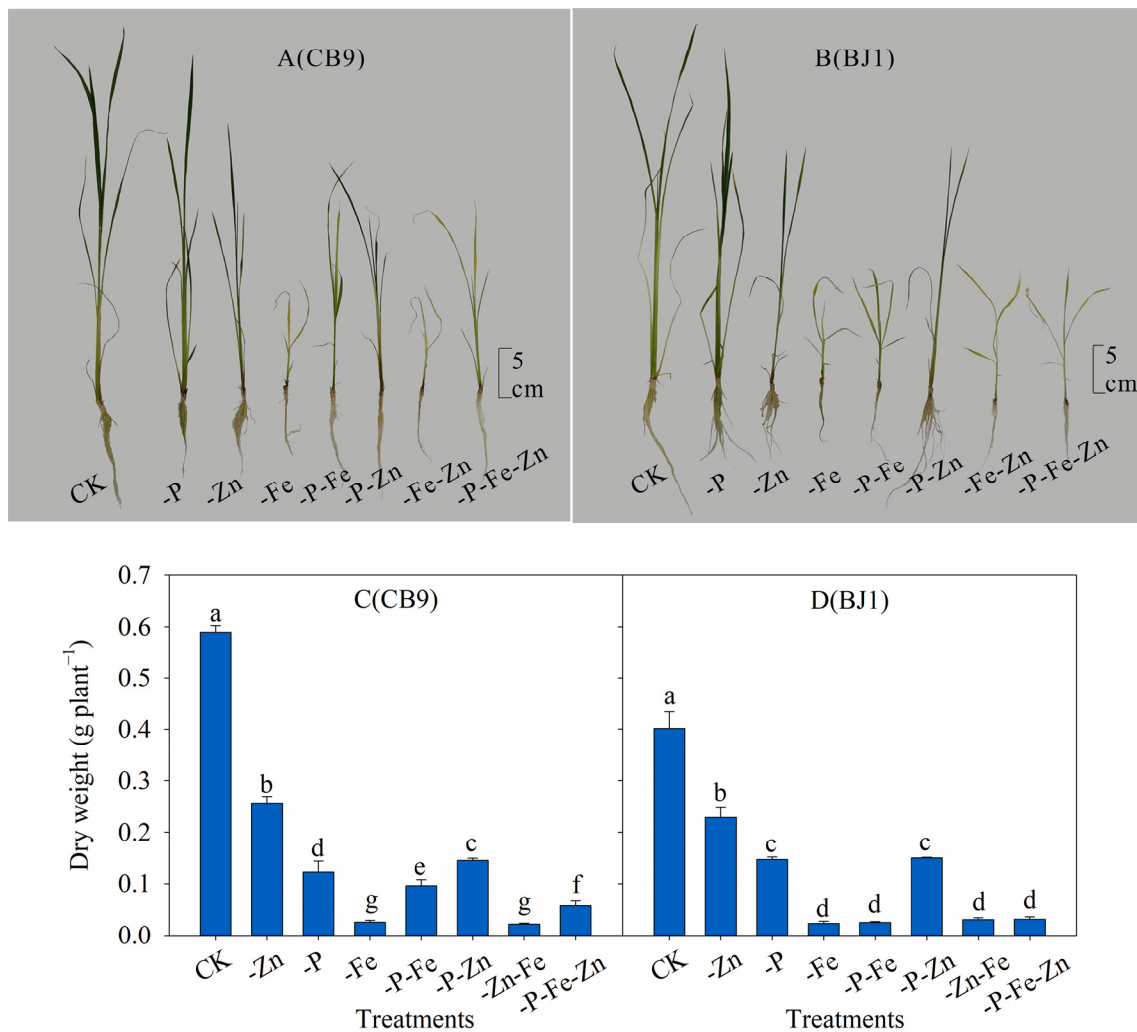


**Figure 1.** Phenotypes (A,B) and dry weight (C,D) of rice seedlings grown for 4 weeks under the deficiency of P, Fe, Zn, and their combinations. Bars represent the mean  $\pm$  SD ( $n = 3$ ). Different lowercase letters on the bars indicate significant differences between treatments of the same cultivar at the  $p < 0.05$  level.

### 3.3. The Rapid A–Ci Response

As shown in Figure 3, the net photosynthetic rate (when stabilized) was inhibited to varying degrees in each deficiency treatment. The -Zn treatment was the least inhibited (especially for the BJ1 cultivar), and the -Fe, -P-Fe, -Zn-Fe, and -P-Fe -Zn treatments were the most inhibited (approximately  $0\text{--}5 \text{ mmol CO}_2 \text{ m}^{-2} \text{ s}^{-1}$ , except for the CB9 cultivar -Fe treatment), which remained consistent for both varieties. The maximum carboxylation efficiency ( $V_{c,max}$ ) and maximum electron transfer rate ( $J_{max}$ ) had the same trend as that of  $P_n$  (when stabilized). Compared with CK, the smallest differences in  $V_{c,max}$  and  $J_{max}$  values were found in the -Zn treatment of both varieties; the largest differences in  $V_{c,max}$  and  $J_{max}$  values were found in the -Fe and -P-Zn-Fe treatments of the CB9 cultivar and the -P-Fe and -Zn-Fe treatments of the BJ1 cultivar. In addition, the  $V_{c,max}$  and  $J_{max}$  values for both varieties showed a trend of  $-\text{Zn} > -\text{P} \geq -\text{P-Zn}$  (a significant difference between the -P-Zn and -P treatments for the BJ1 cultivar). Notably, the effects of the -P, -P-Fe, and -Fe treatments on the  $V_{c,max}$  and  $J_{max}$  values differed slightly between two varieties. The  $V_{c,max}$  and  $J_{max}$  values of the CB9 cultivar showed no significant difference between the -P and -P-Fe treatments but were significantly higher than those of the -Fe treatment. The  $V_{c,max}$  and  $J_{max}$  values of the BJ1 cultivar showed no significant difference between the -P-Fe and -Fe treatments but were significantly lower than those of the -P treatment.

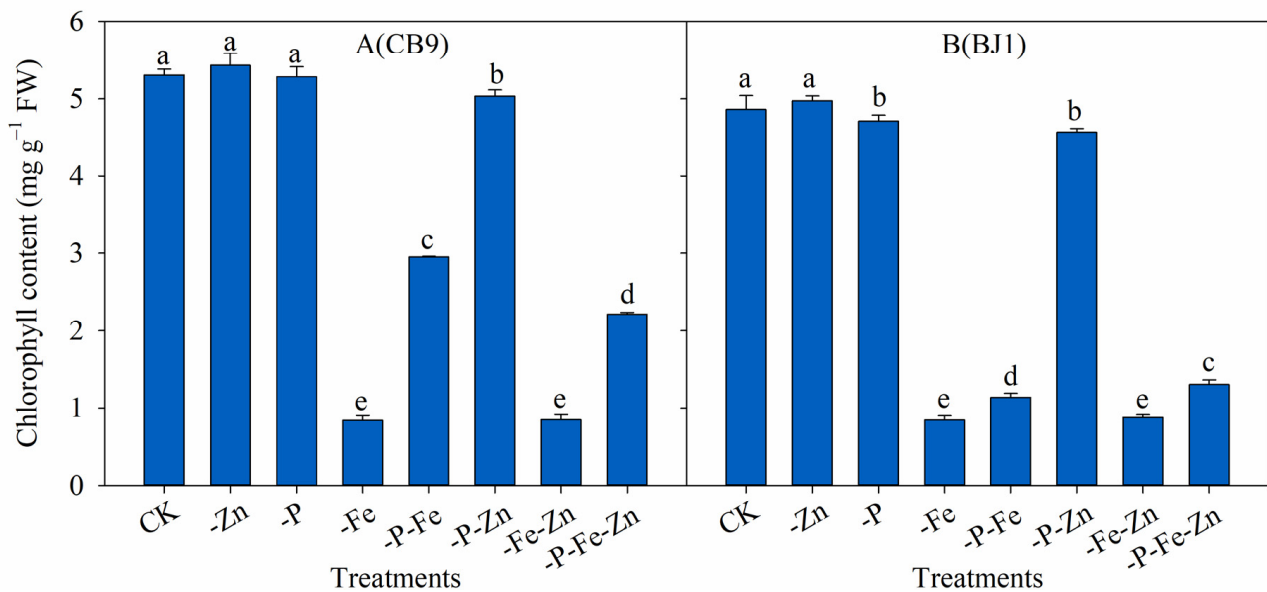


**Figure 2.** Effect of phosphorus, iron, and zinc and their combined deficiencies on total Chl content of rice seedlings. (A,B) are CB9 and BJ1 cultivar, respectively. Bars represent the mean  $\pm$  SD ( $n = 3$ ). Different lowercase letters on the bars indicate significant differences between treatments of the same cultivar at the  $p < 0.05$  level.

### 3.4. Chl *a* Fluorescence Induction Kinetic Curve and JIP-Test Analysis

#### 3.4.1. Chl Fluorescence Induction Kinetics Raw Curve

Figure 4A,C shows the variation in the OJIP curves of rice seedling primordial fluorescence rise kinetics under different element deficiencies and their combinations in the two varieties. The same treatment does not behave in the same manner for both varieties. Compared with CK, the -Zn treatment of the CB9 cultivar increased at point K and decreased at point I but did not affect its  $F_M$  values; and the -P treatment decreased at point J, leading to a decrease in the IP phase, and its  $F_V/F_M$  values were significantly lower than those of the CK treatment. The behavior of the -Zn and -P treatments of the BJ1 cultivar differed: the -Zn treatment increased relative to CK at point K, leading to an increase in FM, and the -P treatment increased at point K, decreased at point I, and reduced its FM value, leading to a significantly lower  $F_V/F_M$  value than that of the CK treatment. In addition, both -Fe and -Zn-Fe in CB9 and BJ1 increased rapidly to maximum fluorescence values equal to  $F_M$  at point K, losing the J-I-P phase, but with lower  $F_M$  values, which also resulted in significantly lower  $F_V/F_M$  values than those of the other treatments (except for the -Fe treatment of the BJ1 cultivar). The -P-Fe treatment of the CB9 cultivar had elevated K and J points but decreased I points, resulting in a decrease in the IP phase. The decrease in J points of the -P-Zn-Fe treatment compared with the CK treatment resulted in a significant decrease in its I point,  $F_M$ , and  $F_V/F_M$ . The -P-Fe and -P-Zn-Fe treatments of the BJ1 cultivar had similar trends to those of -Fe and -Zn-Fe, with both treatments rapidly increasing to  $F_M$ -equivalent maximum fluorescence values at point J and loss of the IP phase. The -P-Fe and -P-Zn-Fe treatments of BJ1 had higher  $F_O$  values relative to -Fe but also relatively elevated  $F_M$  values, resulting in higher  $F_V/F_M$  values than those of the -Fe treatment but significantly lower values than those of the CK treatment. This result suggests that these eight combinations of deficiency treatments differed in their loci of action on the OJIP curve of rice leaf fluorescence rise kinetics, in addition to the cultivar contributing to the loci of action.

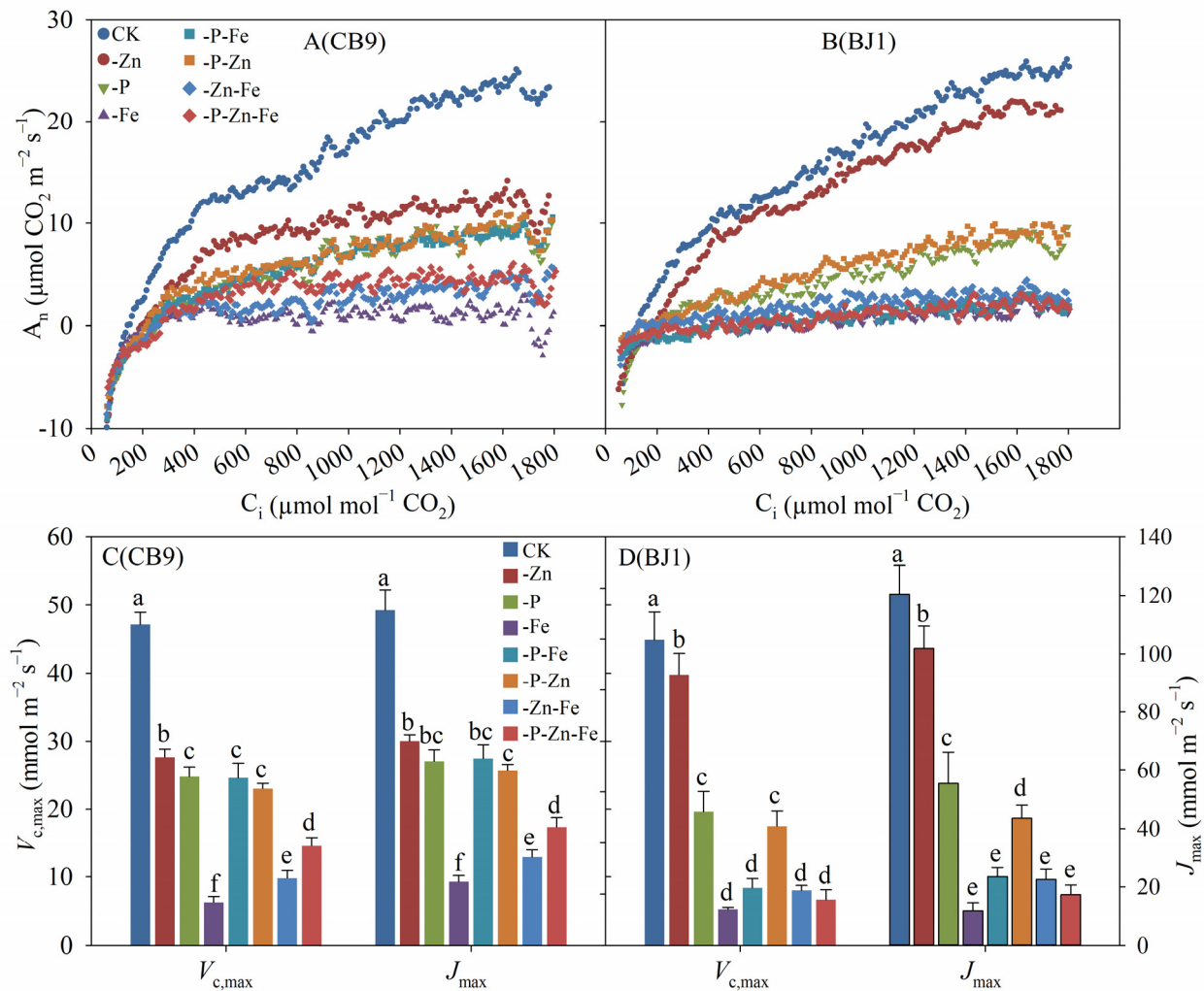


**Figure 3.** Effect of P, Fe, Zn, and their combined deficiencies on the rapid photosynthetic carbon assimilation  $\text{CO}_2$  responses of rice seedlings. (A,B) The A- $C_i$  response curves. (C,D) The maximum carboxylation efficiency ( $V_{c,\text{max}}$ ) and maximum electron transfer efficiency ( $J_{\text{max}}$ ). Bars represent the mean  $\pm$  SD ( $n = 3$ ). Different lowercase letters on the bars indicate significant differences between treatments of the same cultivar at the  $p < 0.05$  level.

### 3.4.2. Standardized Kinetic Curve of Chl Fluorescence

As shown in Figure 5A,C, Chl fluorescence under the -Fe and -Zn-Fe treatments of both varieties, as well as the -P-Fe and -P-Zn-Fe stresses of BJ1, increased significantly at the K step and resulted in a nearly straight line after the J step. By contrast, the K and J steps of the -P-Fe and -P-Zn-Fe treatments of the CB9 cultivar decreased to varying degrees relative to those of CK. In addition, -P, -P-Fe, and -P-Zn-Fe treatments of the CB9 cultivar showed significant  $\Delta J$  and  $\Delta I$  peaks; only the -P and -P-Zn treatments had more pronounced  $\Delta J$  peaks (Figure 3B). For the BJ1 cultivar which appeared to be less sensitive to Zn deficiency than CB9, the curve for the -Zn treatment was nearly identical to that of CK (Figure 3C), whereas the -P-Zn treatment showed distinct  $\Delta J$  and  $\Delta I$  peaks.

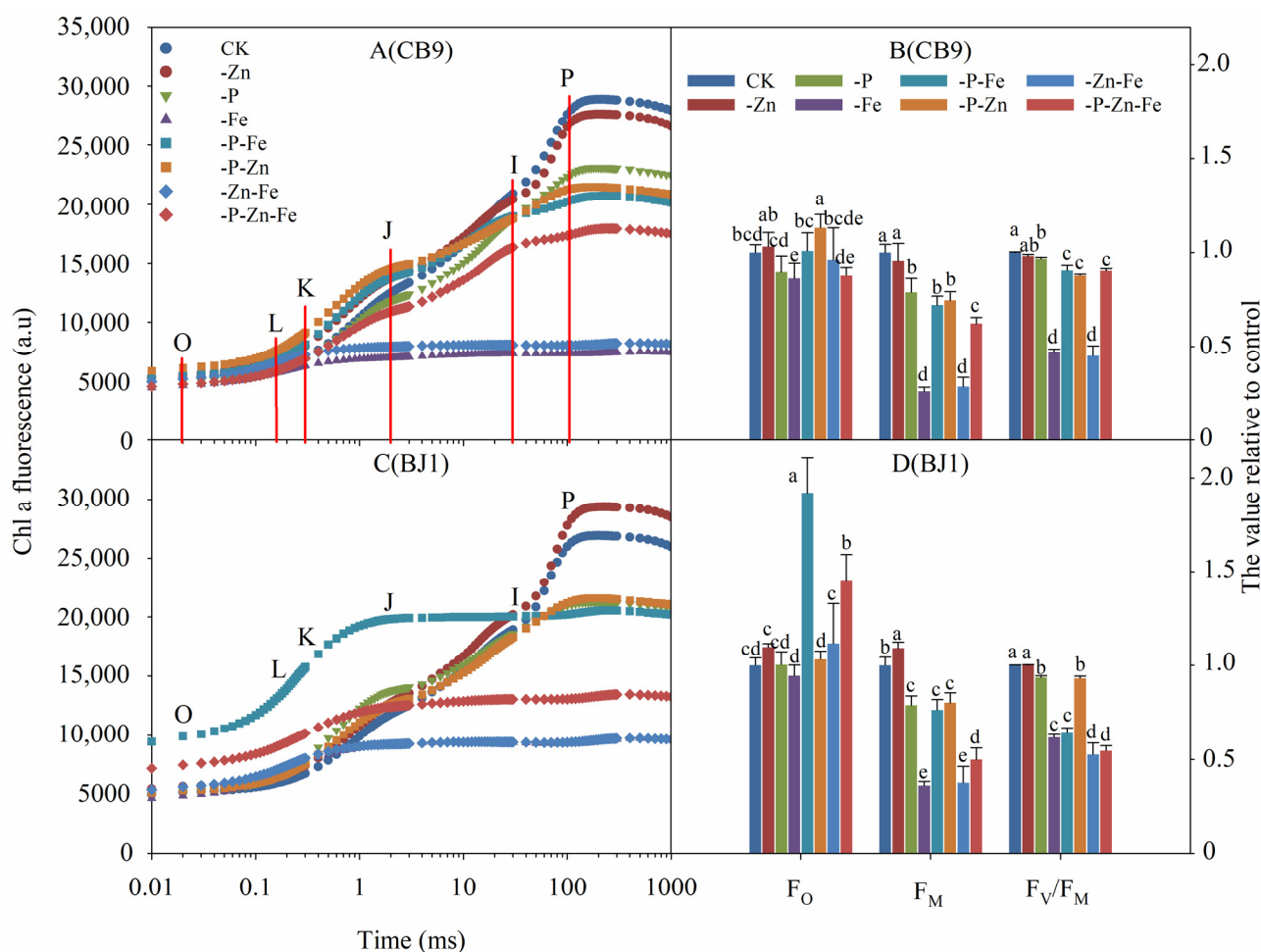


**Figure 4.** Effect of phosphorus, iron, zinc, and their combined deficiencies on the kinetic curve of Chl a fluorescence rise in rice seedlings. **(A,C)** The original Chl fluorescence rise kinetics. Points O, L, K, J, and I represent the fluorescence intensities corresponding to 0.002, 0.15, 0.3, 2, and 30 ms, respectively, and point P represents the maximal fluorescence intensity (generally  $F_P \approx F_M$ ). **(B,D)** The value relative to control of  $F_0$ ,  $F_M$ , and  $F_V/F_M$ . Bars represent the mean  $\pm$  SD ( $n = 6$ ). Different lowercase letters on the bars indicate significant differences between treatments of the same cultivar at the  $p < 0.05$  level.

### 3.4.3. OK Phase

The  $W_{OK}$  (20–300  $\mu s$ , commonly referred to as the L band) is influenced by the transfer of excitation energy between PSII units and is commonly referred to as “connectivity” or “grouping” [29]. As shown in Figure 6A,C, all treatments were significantly different from CK, except for the  $W_L$  of the -Zn and -P treatments of CB9, which were not significantly different from the  $W_L$  of the -Zn and -P-Zn treatments of BJ1, which were not significantly different from CK. This indicates that all other treatments damaged the grouping of leaf PSII units or the energy connectivity between the antennae and PSII reaction center [28]. In addition, the  $W_L$  values of Fe-deficiency-related treatments (-Fe, -P-Fe, -P-Zn-Fe) were all higher and were more pronounced in the BJ1 cultivar than in CB9. However, the P and Fe deficiencies resulted in improved  $W_L$  values in CB9. The change in the  $F_L/F_J$  ratio can assist in determining whether changes in the L band of the fluorescence kinetic curve are caused by changes in the J step. For example, compared with the CK treatment, the -Fe, -P-Fe, -Zn-Fe, and -P-Zn-Fe treatments of the BJ1 cultivar had significantly higher  $W_L$  values but no significant difference in  $F_L/F_J$  values, suggesting that the change in the L band for the -Fe and -P-Zn-Fe treatments of the BJ1 cultivar was caused by an elevated J point.

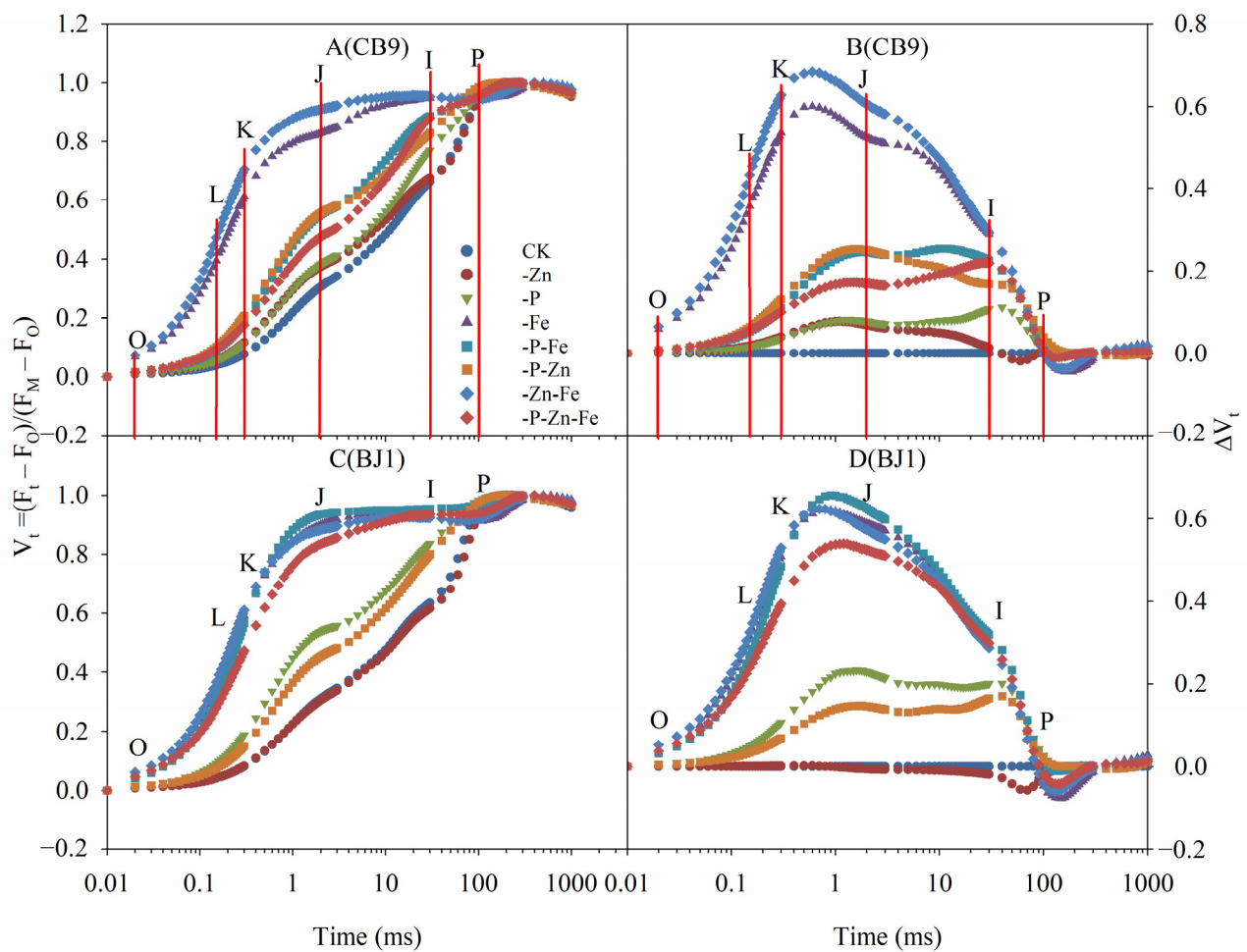


**Figure 5.** Effect of P, Fe, Zn, and their combined deficiencies on the normalized Chl fluorescence rise kinetics OJIP curve ( $V_t$ ) in rice seedlings. (A,C) The normalized Chl fluorescence. (B,D)  $\Delta V_t$ . Points O, L, K, J, and I represent the fluorescence intensities corresponding to 0.002, 0.15, 0.3, 2, and 30 ms, respectively, and point P represents the maximal fluorescence intensity (generally  $F_P \approx F_M$ ).

#### 3.4.4. OJ Phase

The OJ phase (K band) is widely used to indicate the state of the active OEC center on the donor side of PSII, and its appearance is usually associated with the dissociation of the OEC. The  $W_K$  value indicates the degree of impairment in the performance of the donor side of PSII [10,28,30]. As shown in Figure 7, the  $W_K$  values increased significantly for all treatments except for the -Zn treatment of the BJ1 cultivar. This indicates that all treatments except the -Zn treatment of BJ1 caused partial inactivation of the oxygen-emitting complex (OEC) on the donor side of PSII, evidenced by the reduction in OEC relative activity [OEC] values [28]. Among the treatments, the -Zn-Fe and -Fe treatments of the CB9 cultivar and the -P-Fe, -P-Zn-Fe, -Zn-Fe, and -Fe treatments of the BJ1 cultivar caused the greatest damage to the OEC on the PSII donor side of the treatment. In contrast with CK, the -Zn, -P, and -Zn treatments of CB9 showed a significant increase in  $F_K/F_J$ , and the  $W_K$  values did not change significantly. This suggests that the increase in the OJ phase of the -Zn, -P, and -Zn treatments of CB9 and BJ1 was caused by an increase in point J.

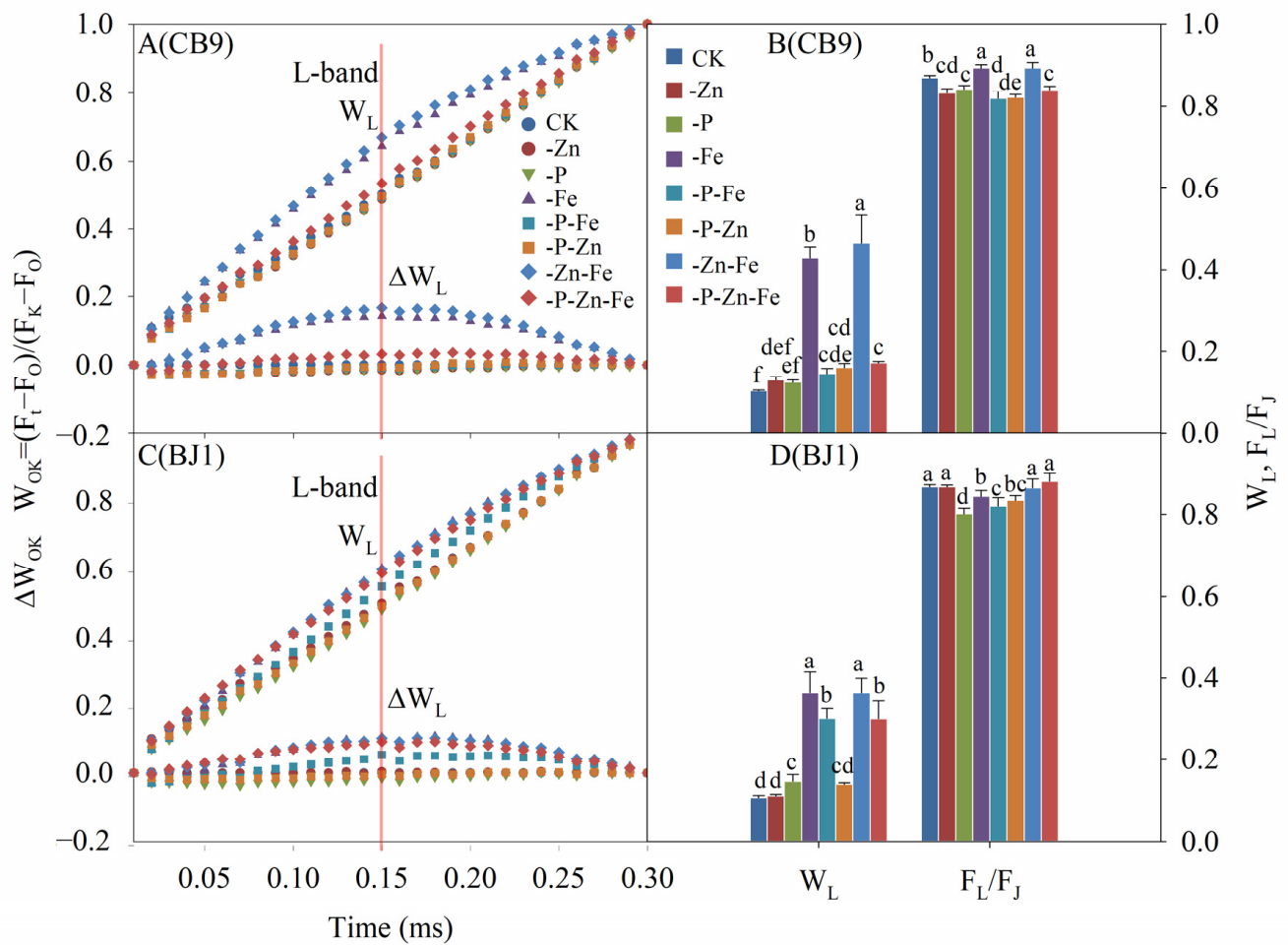


**Figure 6.** Effect of P, Fe, Zn, and their combined deficiencies on the OK phase of standardized Chl fluorescence rise kinetics in rice seedlings. (A,C) Variable fluorescence between the steps O and K  $W_{OK}$ ;  $\Delta W_{OK}$ . (B,D) The value of  $W_L$ , and  $F_L/F_J$ ;  $W_L$ , relative variable fluorescence at the L step to the amplitude  $F_K - F_O$  ( $W_L$ ). Bars represent the mean  $\pm$  SD ( $n = 6$ ). Different lowercase letters on the bars indicate significant differences between treatments of the same cultivar at the  $p < 0.05$  level.

### 3.4.5. OI Phase

The maximum amplitude of the  $W_{OI}$  curve reflects information on the pool size of the terminal electron acceptor on the PSI receptor side. As shown in Figure 8A,C, P, Fe, Zn, and their combined deficiencies had significantly different effects compared with CK (except for the -Zn treatment). The lower the amplitude, the stronger the suppression of the pool size. The difference between  $W_{IP}$  and CK was smallest for CB9 treated with -Zn, indicating that -Zn had the least effect on the pool of electron acceptors at the end of PSI. By contrast, the -Fe and -P-Zn-Fe treatments of CB9 differed the most from the -Fe, -P-Zn-Fe, -P-Fe, and -Zn-Fe treatments of BJ1 from CK, and the -P-Zn-Fe and -P-Fe treatments had  $W_{IP}$  values less than 1 and the least inhibition of the pool of PSI-terminal electron acceptors.

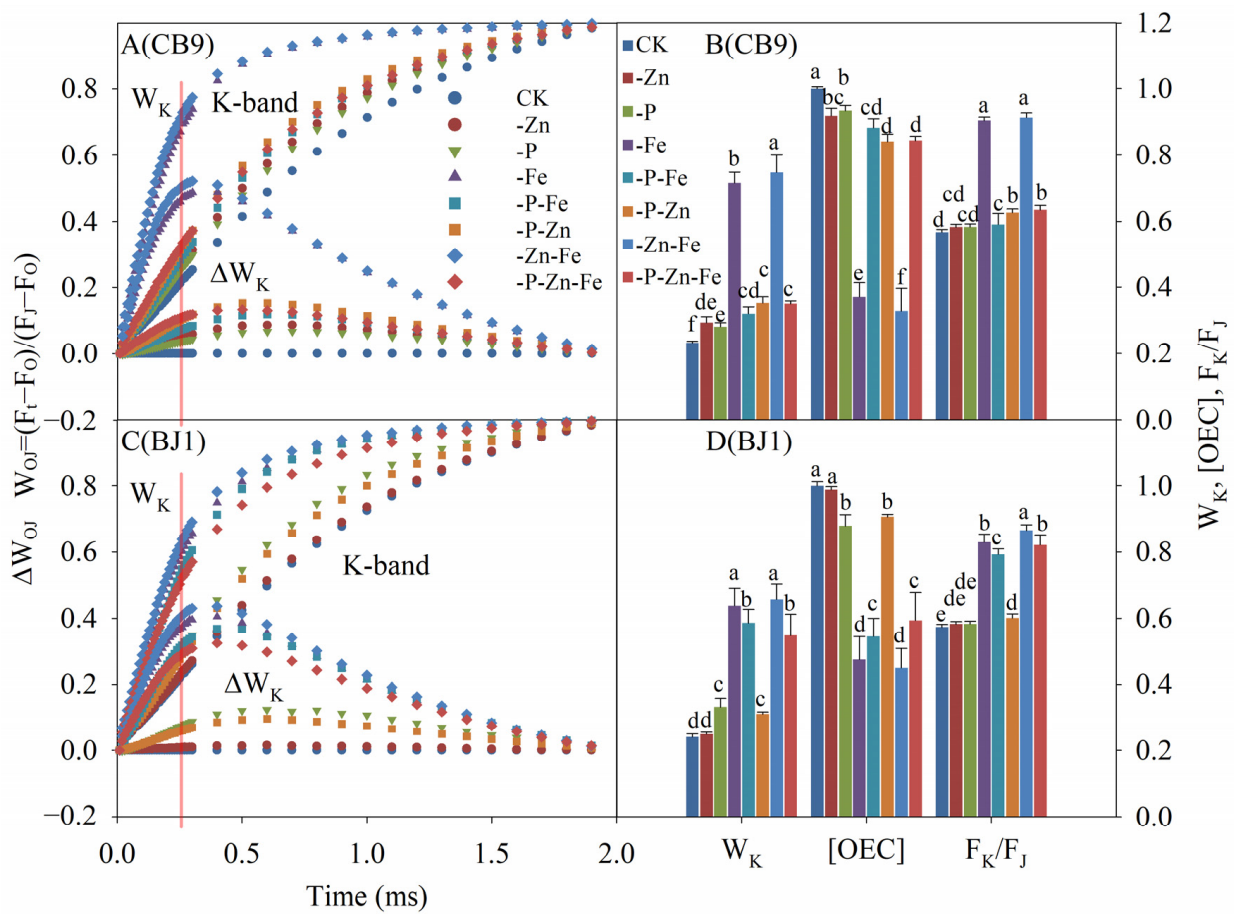


**Figure 7.** Effect of P, Fe, Zn, and their combined deficiencies on the OJ phase of standardized Chl fluorescence rise kinetics in rice seedlings. (A,C) Variable fluorescence between the steps O and J ( $W_{OJ}$ );  $\Delta W_{OJ}$ . (B,D) The value of  $W_K$ , [OEC], and  $F_K/F_J$ ;  $W_K$ , relative variable fluorescence at the K step to the amplitude  $F_J - F_O$  ( $W_K$ ); [OEC], the active fraction of OEC centers and can be calculated by  $[OEC] = [1 - (V_K/V_J)_{treatment}]/[1 - (V_1/V_J)_{CK}]$ . Bars represent the mean  $\pm$  SD ( $n = 6$ ). Different lowercase letters on the bars indicate significant differences between treatments of the same cultivar at the  $p < 0.05$  level.

### 3.4.6. Specific Fluxes Membrane Model

The specific fluxes membrane model (Figure 9) reflects the energy flux per the reflective center of the primary response of rice seedling leaves in the absence of P, Fe, Zn, or their combinations. As shown in Figure 9, the unit reaction centers of the two rice varieties showed higher energy absorption ( $ABS/RC$ ) and energy capture ( $TR_0/RC$ ) than that with CK, except for the -Zn treatment and the -P treatment of the CB9 cultivar. Most of this energy is dissipated ( $DI_0/RC$ ) through the exotherm, and less energy is used for transfer ( $ET_0/RC$ ). This is not only related to the disruption of the electron transport chain but also to the activity of the unit reaction center ( $RC/ABS$ ) (Table 1). This results also in the low flux of electrons from the individual active reaction centers to the PSI-terminal electron acceptor for its reduction. The energy distribution among the treatments was uneven for the -Fe, -Fe-Zn, -P-Fe, and -P-Fe-Zn treatments of the BJ1 cultivar, with the -Fe-Zn treatment being the most severe in both varieties. In addition, the -P-Fe and -P-Fe-Zn treatments had opposite effects on the two rice varieties. In the CB9 cultivar, the -P-Fe and -P-Fe-Zn treatments were observed to improve the energy flux profile of each reaction center under the -Fe treatment; in the BJ1 cultivar, this effect was absent. This result may be related to cultivar characteristics.

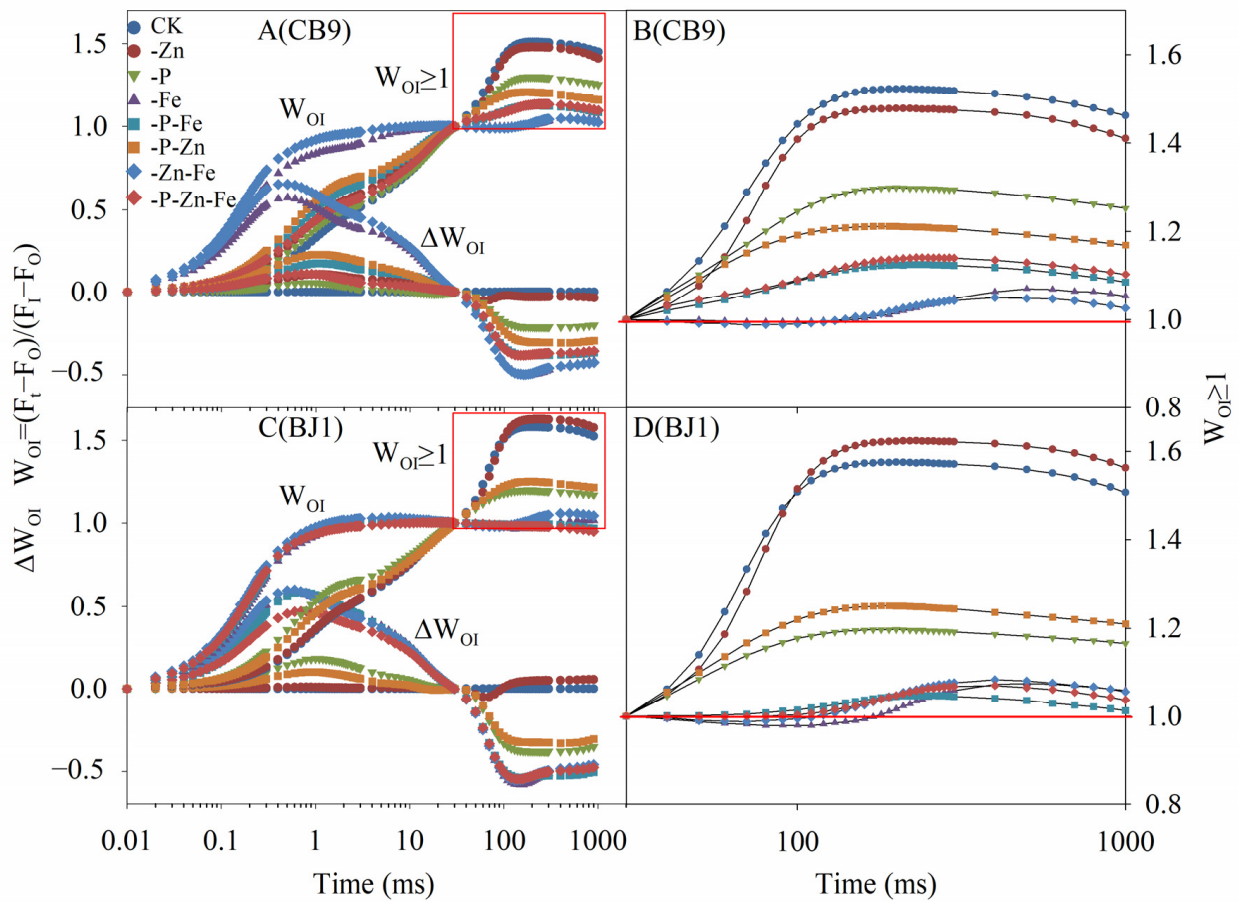


**Figure 8.** Effect of P, Fe, and Zn and their combined deficiencies on the OI phase of chlorophyll fluorescence in rice seedlings. (A,C) Variable fluorescence between the steps O and I ( $W_{OI}$ ),  $\Delta W_{OI}$ . (B,D)  $W_{OI} \geq 1$ .

### 3.4.7. Important Parameters of the Photosystem

Table 1 shows that P, Fe, and Zn deficiencies and their combinations adversely affected parameters such as quantum yield, flux ratio, and the performance index  $PI_{ABS}$  in rice seedlings. Compared with CK, the -Zn treatment of both rice varieties maintained higher PSII active reaction center concentrations (RC/ABS) and had the least effect on the quantum yield ( $\varphi_{P_0}$ ,  $\varphi_{E_0}$ , and  $\varphi_{R_0}$ ) and flux ratios ( $\psi_{E_0}$ ,  $\psi_{R_0}$ , and  $\delta_{R_0}$ ) of the primary photochemical reactions, maintaining a higher performance index ( $PI_{ABS}$ ) than the other deficiency treatments. While the -P treatment maintained a high  $\varphi_{P_0}$ , the electron transfer from  $Q_A$  to electron acceptors other than  $Q_A$  and the electron reduction in the terminal electron acceptors on the PSI acceptor side were somewhat impaired, leading to a decrease in their quantum efficiency, flux ratio, and  $PI_{ABS}$  values. The overall performance of the -P-Zn treatment was similar to that of the -P treatment but with somewhat more severe damage to the electron transfer chain. The -Fe and -Fe-Zn treatments severely disrupted the electron transport chain of photosynthesis, significantly reducing parameters such as the quantum yield and flux ratio, leading to a significant increase in the heat dissipation efficiency to protect the photosynthetic organs of rice seedlings. The two aforementioned treatments had slightly different effects on parameters such as the quantum yield and flux ratio of the electron transport chain in the two rice varieties, but the overall trends converged. However, the effects of the -P-Fe and -P-Fe-Zn treatments on the quantum yield, flux ratio, and  $PI_{ABS}$  of the two rice varieties differed; the performance of the CB9 cultivar was significantly better than that of the BJ1 cultivar.

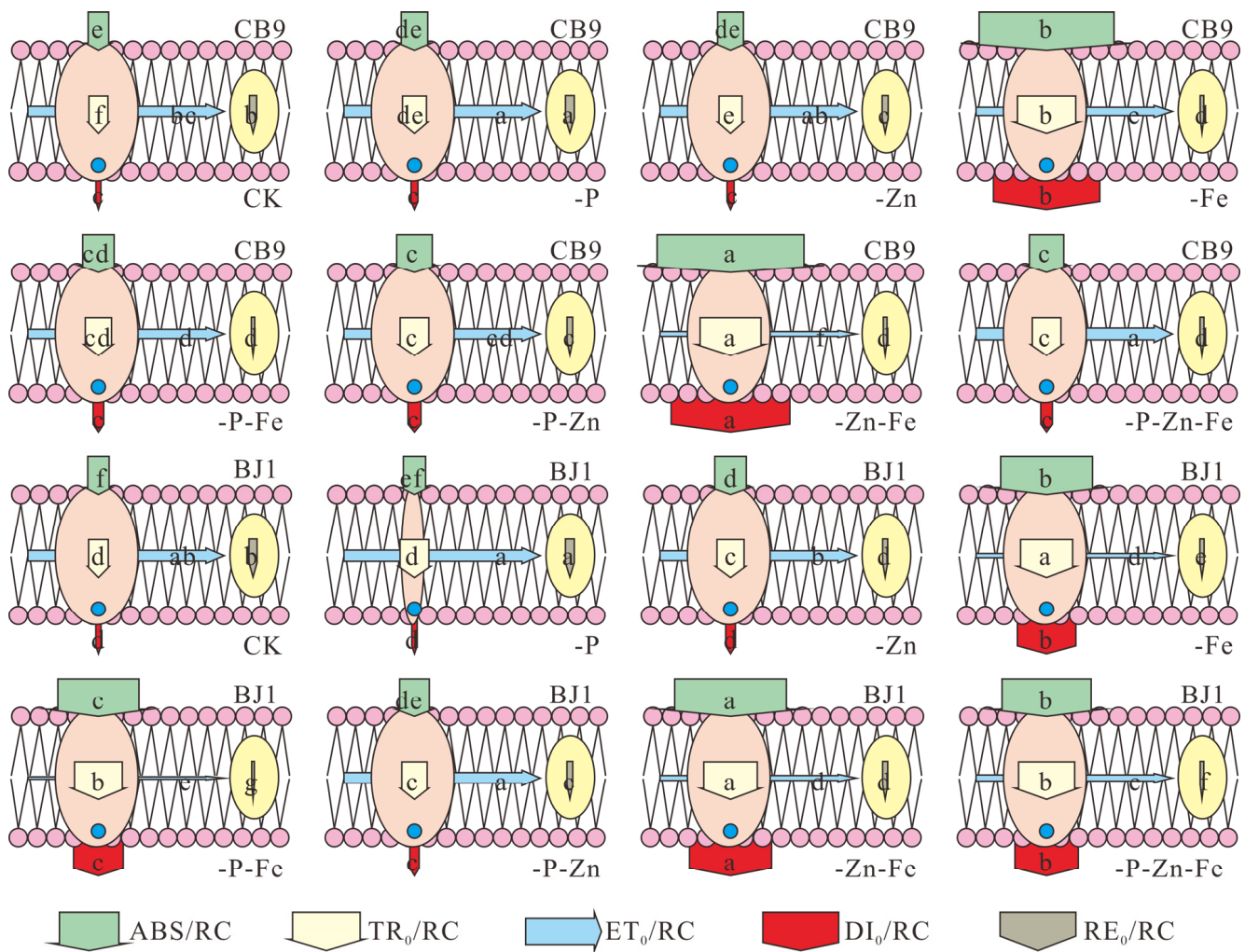


**Figure 9.** Effect of P, Fe, and Zn and their combined deficiencies on the specific fluxes membrane model in rice seedlings. ABS/RC: Absorbed photon flux per active PSII. TR<sub>0</sub>/RC: Trapped energy flux per active PSII. ET<sub>0</sub>/RC: Electron flux from Q<sub>A</sub><sup>-</sup> to the PQ pool per active PSII. DI<sub>0</sub>/RC: Dissipated energy (as heat and fluorescence) flux per active PSII. RE<sub>0</sub>/RC: Electron flux from Q<sub>A</sub><sup>-</sup> to the final electron acceptors of PSI per active PSII. Note: The model has been slightly modified and we have added the indicator RE<sub>0</sub>/RC. Bars represent the mean ± SD (n = 6). Different lowercase letters on the same symbol indicate significant differences between treatments of the same cultivar at the p < 0.05 level.

### 3.5. Correlation between Growth Parameters and Photosynthesis-Related Indicators

As shown in Figure 10, the dry matter of rice seedlings was significantly correlated with photosynthesis-related indicators such as total Chl content, V<sub>c,max</sub>, J<sub>max</sub>, quantum yield (φ<sub>P0</sub>, φ<sub>E0</sub>, and φ<sub>R0</sub>), flux ratios (ψ<sub>E0</sub>, ψ<sub>R0</sub>), RC/ABS, and PI<sub>ABS</sub>. All indicators in Figure 10 show a highly significant positive correlation, except for the heat dissipation ratio (φ<sub>D0</sub>), which shows a highly significant negative correlation with the other indicators. Both varieties were consistent.

**Table 1.** Effect of P, Fe, and Zn and their combined deficiencies on important parameters of the photosystem of rice leaves.

Cultivar	Treatments	$F_O/F_V$	$\varphi_{P_0}$	$\varphi_{E_0}$	$\varphi_{D_0}$	$\varphi_{R_0}$	$\psi_{E_0}$	$\psi_{R_0}$	$\delta_{R_0}$	RC/ABS	PI <sub>ABS</sub>
CB9	CK	5.32 ± 0.10 a	0.81 ± 0.00 a	0.57 ± 0.01 a	0.19 ± 0.00 d	0.28 ± 0.01 a	0.70 ± 0.01 a	0.34 ± 0.02 a	0.49 ± 0.02 ab	0.87 ± 0.02 a	8.88 ± 0.48 a
	-Zn	4.92 ± 0.17 b	0.80 ± 0.01 ab	0.50 ± 0.01 b	0.20 ± 0.01 cd	0.26 ± 0.02 b	0.63 ± 0.01 b	0.33 ± 0.03 a	0.52 ± 0.04 a	0.68 ± 0.04 b	4.58 ± 0.34 b
	-P	4.66 ± 0.13 c	0.79 ± 0.01 b	0.49 ± 0.00 c	0.21 ± 0.01 c	0.18 ± 0.01 c	0.62 ± 0.01 b	0.23 ± 0.01 b	0.37 ± 0.02 c	0.70 ± 0.03 b	4.21 ± 0.28 c
	-Fe	1.62 ± 0.04 f	0.38 ± 0.01 d	0.07 ± 0.01 g	0.62 ± 0.01 a	0.02 ± 0.00 f	0.18 ± 0.02 e	0.05 ± 0.01 e	0.30 ± 0.07 cd	0.13 ± 0.01 e	0.02 ± 0.00 g
	-P-Fe	3.81 ± 0.31 d	0.74 ± 0.02 c	0.34 ± 0.01 e	0.26 ± 0.02 b	0.08 ± 0.01 e	0.46 ± 0.02 d	0.11 ± 0.02 d	0.25 ± 0.04 d	0.57 ± 0.05 c	1.36 ± 0.21 d
	-P-Zn	3.49 ± 0.07 e	0.71 ± 0.01 c	0.32 ± 0.01 f	0.29 ± 0.01 b	0.12 ± 0.01 d	0.45 ± 0.01 d	0.17 ± 0.01 c	0.38 ± 0.02 bc	0.50 ± 0.02 d	1.04 ± 0.07 f
	-Fe-Zn	1.59 ± 0.11 f	0.37 ± 0.04 d	0.04 ± 0.01 h	0.63 ± 0.04 a	0.02 ± 0.01 f	0.10 ± 0.02 f	0.05 ± 0.02 e	0.55 ± 0.21 a	0.12 ± 0.01 e	0.01 ± 0.00 g
	-P-Fe-Zn	3.77 ± 0.16 d	0.73 ± 0.01 c	0.39 ± 0.00 d	0.27 ± 0.01 b	0.09 ± 0.01 e	0.53 ± 0.01 c	0.12 ± 0.02 d	0.23 ± 0.03 d	0.52 ± 0.02 d	1.66 ± 0.05 e
BJ1	CK	5.22 ± 0.03 a	0.81 ± 0.00 a	0.56 ± 0.01 a	0.19 ± 0.00 d	0.30 ± 0.02 b	0.70 ± 0.01 a	0.37 ± 0.02 b	0.53 ± 0.03 b	0.84 ± 0.03 a	8.14 ± 0.64 a
	-Zn	5.20 ± 0.10 a	0.81 ± 0.00 a	0.57 ± 0.01 a	0.19 ± 0.00 d	0.31 ± 0.01 a	0.70 ± 0.01 a	0.39 ± 0.01 a	0.55 ± 0.02 b	0.81 ± 0.02 b	8.02 ± 0.60 a
	-P	4.11 ± 0.12 b	0.76 ± 0.01 b	0.35 ± 0.01 c	0.24 ± 0.01 c	0.13 ± 0.01 d	0.47 ± 0.01 c	0.17 ± 0.01 d	0.36 ± 0.02 c	0.57 ± 0.04 d	1.56 ± 0.14 c
	-Fe	2.00 ± 0.05 c	0.50 ± 0.01 c	0.05 ± 0.00 e	0.50 ± 0.01 b	0.04 ± 0.01 e	0.11 ± 0.01 e	0.07 ± 0.01 e	0.68 ± 0.10 a	0.20 ± 0.02 e	0.02 ± 0.00 d
	-P-Fe	2.08 ± 0.09 c	0.52 ± 0.02 c	0.04 ± 0.00 f	0.48 ± 0.02 b	0.03 ± 0.00 e	0.07 ± 0.01 f	0.05 ± 0.01 f	0.70 ± 0.10 a	0.22 ± 0.01 e	0.02 ± 0.00 d
	-P-Zn	4.06 ± 0.15 b	0.75 ± 0.01 b	0.42 ± 0.01 b	0.25 ± 0.01 c	0.15 ± 0.02 c	0.55 ± 0.02 b	0.20 ± 0.02 c	0.37 ± 0.03 c	0.61 ± 0.01 c	2.29 ± 0.17 b
	-Fe-Zn	1.75 ± 0.15 d	0.43 ± 0.05 d	0.05 ± 0.00 e	0.57 ± 0.05 a	0.04 ± 0.01 e	0.12 ± 0.02 e	0.08 ± 0.01 e	0.71 ± 0.17 a	0.16 ± 0.02 f	0.02 ± 0.00 d
	-P-Fe-Zn	1.80 ± 0.07 d	0.44 ± 0.02 d	0.08 ± 0.01 d	0.56 ± 0.02 a	0.03 ± 0.00 e	0.18 ± 0.03 d	0.07 ± 0.01 e	0.41 ± 0.07 c	0.20 ± 0.03 e	0.04 ± 0.00 d

$F_O/F_V$ : the ratio of photochemical to non-photochemical quantum efficiency.  $\varphi_{P_0}$ : maximum quantum yield for primary photochemistry.  $\varphi_{E_0}$ : quantum yield for electron transport (ET).  $\varphi_{D_0}$ : quantum yield (at  $t = 0$ ) of energy dissipation.  $\varphi_{R_0}$ : quantum yield for reduction of the end electron acceptors at the PSI acceptor side (RE).  $\psi_{E_0}$ : efficiency with which a PSII trapped electron is transferred from  $Q_A^-$  to PQ.  $\psi_{R_0}$ : efficiency with which a PSII trapped electron is transferred to final PSI acceptors.  $\delta_{R_0}$ : probability that an electron is transported from the reduced intersystem electron acceptors to the final electron acceptors of PSI (RE). RC/ABS: reflects PSII active reaction center concentration. PI<sub>ABS</sub>: performance index (potential) for energy conservation from photons absorbed by PSII to the reduction in intersystem electron acceptors. Means ± SD are shown ( $n = 6$ ). Different lowercase letters in the same column on the table indicate significant differences between treatments of the same cultivar at the  $p < 0.05$  level.

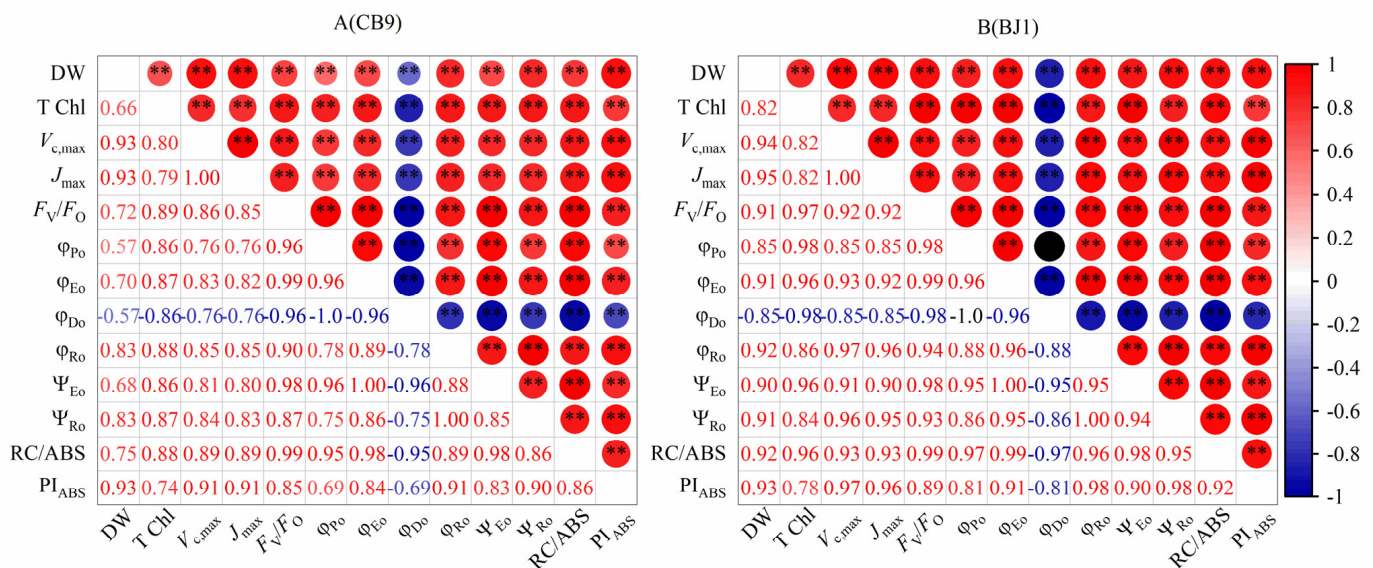


**Figure 10.** Pearson’s correlation of rice seedling growth parameters with photosynthesis-related indicators (n = 3). (A,B) are CB9 and BJ1 cultivar, respectively. \*\* indicates a significant difference at the level of  $p < 0.01$ .

#### 4. Discussion

An effective supply of nutrients is essential for plant growth and development; however, deficiencies and imbalances of nutrients are common in plant growth. Research on nutrient deficiencies has focused on single nutrients, and in addition to limiting plant growth, single-element deficiencies are often accompanied by specific biological phenomena [4,15]. For example, the plants are short, thin, and tufted (-P); have shortened leaf-pillow spacing (-Zn); and the leaves are fading green (-Fe) (Figure 1A,B). Chl a fluorescence is a probe for the study of photosynthesis, and information on the photosynthetic electron transport chain can be obtained from Chl fluorescence-induced kinetic curves, using Chl fluorescence to identify and assess single deficiencies of multiple nutrients in maize, tomato, and oilseed rape plants [10,31–34]. These studies demonstrate the effectiveness of the Chl fluorescence technique in identifying plant nutrient deficiencies. This study is the first attempt to use JIP-test analysis to explore the effects of P, Fe, Zn, and their combined deficiency on photosystem II performance in rice. The limitation of photosynthetic carbon assimilation was explored to improve the understanding of the effect of elemental combination deficiency on photosynthetic properties of rice seedlings. Nutrient deficiencies can directly or indirectly cause changes in plant growth and development. These changes are thought to explore adaptive strategies for improving access to deficient elements, but the physiological and biological relevance to plants when deficient in one or more elements is still poorly understood [19]. Chaiwong et al. [4] found that P, Fe, and their combination deficiency all reduced the fresh weight of rice seedlings (SPR1 varieties). Saenchai et al. [35] found that -Fe, -P-Fe, -P-Zn, -Fe-Zn, and -P-Fe-Zn all reduced the dry weight of rice seedlings, -P had no effect on dry weight, and -Zn significantly increased it. In this study, the deficiency of P, Fe, Zn, and their different combinations resulted in different changes in the dry weight of rice seedlings, which was not entirely consistent with previous studies. This may be related to the cultivar of rice. Overall, iron deficiency had the strongest single nutritional impact on rice seedling biomass, and zinc deficiency had the weakest ability to limit rice seedling biomass. Saenchai et al. [35] also concluded that iron deficiency has the strongest single nutritional impact on biomass. This could be due to -Fe-induced chlorosis, which limits photosynthesis as well as dry matter accumulation. Additionally, the latest studies suggest that -Fe-induced yellowness is based on the presence of P, which further supports the results of our experiments [12]. However, the -Zn, -P, and -P-Fe (CB9 cultivar) treatments did not significantly reduce total Chl content. This may be due to the fact

that P, Fe, and Zn have different transit pathways and different interactions between the elements, different demand times, and different roles in various physiological metabolic pathways, such as photosynthesis and the antioxidant system in rice, but elemental deficiencies all cause varying degrees of disruption to normal rice metabolism [12,15,16,24]. In most cases, simultaneous deficiencies of multiple elements are more harmful to plants than single-element deficiencies [19]. For example, the -Fe-Zn-treated rice seedlings in the two varieties in this trial performed worse or insignificantly relative to the -Zn or -Fe treatments. This may be due to the extensive involvement of Fe and Zn in the synthesis of antioxidant enzymes and in the redox processes of the enzymes of glutathione metabolism, with the simultaneous deficiency of both causing greater damage to the plant antioxidant system than the individual deficiencies [16,36]. However, some studies have found that deficiencies in both elements may alleviate the harm caused by a single-element deficiency. For example, -P-Fe-treated plants can alleviate the limitations caused by Fe deficiency [4,35]. Similar results were observed in this study. The growth performance of rice seedlings in the -P-Fe and -P-Fe-Zn treatments was significantly better than that in the -Fe treatment in the CB9 cultivar, and the dry matter performance of both types of rice seedlings in the -P-Zn treatment was better than that in the -P treatment. However, the mitigating effect of -P-Fe on -Fe was not evident in BJ1. This may be because the interaction between the elements is also somewhat related to cultivar and may be related to the various sensitivities of the cultivar to the elements.

Because P, Fe, Zn, and their combined deficiency limit photosynthetic carbon assimilation ( $V_{c,max}$ ,  $J_{max}$ , and the maximum net photosynthetic rate at stability were all reduced, Figure 3) in seedling leaves to varying degrees, Chl fluorescence was measured in rice seedlings to improve the understanding of the effects of each deficiency on photosynthetic properties.  $F_V/F_M$  can be used as an indicator of photoinhibition, reflecting the maximum quantum yield of the primary photochemistry [37]. Kalaji et al. [33] found that -Fe and -Zn reduced the  $F_V/F_M$  values of maize and tomato but -P did not significantly reduce the  $F_V/F_M$  values.  $F_V/F_M$  and the ratio of photochemical to non-photochemical quantum efficiency ( $F_V/F_O$ ) in this study showed the same trend (Figure 4B,D, Table 1), indicating that all treatments (except -Zn) caused photoinhibition of the uppermost spreading leaves of rice seedlings [38]. However, the overall photosynthetic characteristics ( $V_{c,max}$ ,  $J_{max}$ , Figure 3C,D) of -Zn treated rice seedlings were inhibited, along with the morphology and dry matter (Figure 1). This may be because, under -Zn treatment, rice transports Zn elements from the older leaves to the newer leaves [39], resulting in the uppermost unfurling leaves not showing significant photoinhibition.

Standardized fluorescence kinetic curves can reflect the implicit features of Chl fluorescence rise kinetic OJIP curves and quantify PSII behavior/activity using JIP-test analysis [28]. To describe the effect of the lack of -P, -Fe, -Zn, and their combinations on Chl fluorescence kinetics in detail, we analyzed the normalized fluorescence kinetic curves in phases. The presence of a positive  $W_{OK}$  (L band, Figure 6A,C) indicates weak connectivity between adjacent PSII at the level of the antenna complex [40]. In this study, all other treatments (except the -Zn treatment as well as the -P treatment for CB9 species and the -P-Zn treatment for BJ1 species) reduced the connectivity of PSII antenna complexes. The -Fe and -Zn-Fe treatments of the two varieties and -P-Fe and -P-Fe-Zn treatments of the BJ1 cultivar caused the greatest disruption to the connectivity of the PSII antenna complex. Elemental deficiencies may affect the structure of vesicle-like membranes and reduce the transfer of excitation energy between adjacent photosynthetic units [40]. Further analysis of the K points showed that all treatments (except for the BJ1 cultivar) were limited in their performance on the donor side, especially the -Fe and -Fe-Zn treatments for both varieties and the -P-Fe and -P-Fe-Zn treatments for the BJ1 cultivar, which were the most limiting in their performance on the donor side. Part of the reason for this result is due to nutrient deficiencies and partial inactivation of the OEC, reducing the rate of electron transfer on the donor side [31,34]. The extent of damage to the OEC was also supported by the reduction in  $[OEC]$  (Figure 7B,D). Another part of the cause may be due to the accumulation of reac-

tive oxygen species caused by electron leakage due to the inhibition of PSII electron flow outside  $Q_A$  [30]. In addition, the -Fe and -Fe-Zn treatments of two varieties and the -P-Fe and -P-Fe-Zn treatments of the BJ1 cultivar damaged the PSII receptor side performance ( $V_j$ ) more severely than treatments such as -P and -P-Zn. This is also evidenced by the reduction in  $\varphi_{E_0}$  and  $\psi_{E_0}$ . This not only leads to an amplitude reduction close to 1 for  $W_{OI} \geq 1$  but also to the near disappearance of the IP phase (Figure 8B,D). This suggests that the aforementioned treatment not only leads to a reduction or disruption of the electron acceptor pool at the end of the PSI receptor side but also breaks electron transport beyond  $Q_A$  in the PSII electron transport chain [30]. This probably occurs because Zn is a structural stabilizer, and Fe is an essential metal with redox activity [16]. Zn or Fe deficiency can damage the electron acceptor pool, which may also be related to the characteristics of the cultivar [4,20,41]. Studies have shown that -P-Fe can mitigate damage caused by -Fe [35]. However, in this study, the two varieties did not perform equally well against simultaneous P and Fe combined deficiency, with the -P-Fe treatment of CB9 performing significantly better than -Fe. By contrast, the differences between the -P-Fe and -Fe treatments of the BJ1 cultivar were nonsignificant, probably because of the cultivar.

The membrane model reflects the energy flow per reaction center in PSII. Further analysis of the biofilm energy flow revealed that prolonged vegetation-deficient incubation led to the deactivation of some reaction centers (lower RC/ABS, Table 1), increasing the energy absorbed and captured per reaction center (Figure 9). Under -Fe, -Fe-Zn, and BJ1 species of -P-Fe and -P-Fe-Zn treatments, more energy is absorbed by each reaction center, but less of this energy is used for transfer and most of it is used for heat dissipation (Figure 9). This enhancement of heat dissipation by regulating the deactivation of reaction centers, which allows leaves to reduce photo-oxidative damage and avoid excessive light energy absorption, is a self-protective mechanism in plant photosynthesis [34]. This is the main reason for the reduction in energy capture, transfer efficiency, and  $RE_0/RC$  values. In particular, the values of  $\varphi_{P_0}$ ,  $\varphi_{E_0}$ ,  $\psi_{E_0}$ , and  $\delta_{R_0}$  were significantly lower (Table 1), suggesting that the PQ exchange capacity at the  $Q_B$  site and the PQH2 reoxidation capacity were reduced, and the quantum yield for electron transfer from both  $Q_A^-$  to the electron transfer chain beyond  $Q_A^-$  and from  $Q_A^-$  to the reduced electron acceptor at the end of the PSI receptor side was severely limited [37].

$PI_{ABS}$  reflects the overall performance of PSII. It is generated from three components:  $\gamma_{RC}/(1 - \gamma_{RC})$  (PSII active reaction center concentration,  $\gamma_{RC}/(1 - \gamma_{RC}) = RC/ABS$ ),  $\varphi_{P_0}/(1 - \varphi_{P_0})$  (primary photochemical reactions), and  $\varphi_{E_0}/(1 - \varphi_{E_0})$  (electronic transmission). Any significant decrease in the  $PI_{ABS}$  values can be attributed to changes in these three parameters [42]. Kalaji et al. [33] considered in a single-nutrient deficiency diagnosis study using chlorophyll fluorescence parameters in maize and tomato that  $PI_{ABS}$  and  $PI_{total}$  (a measure for the performance up to the reduction of PSI end-electron acceptors) could reflect the response to nutrient deficiency in both species, and especially  $PI_{total}$  could be used as a parameter to monitor the effect of nutrient deficiency on PSI. Our data suggest that in this study, although  $PI_{ABS}$  decreased to varying degrees for each of the deficiency treatments, the reasons for the decrease varied. By comparing the magnitude of the reduction in these three parameters, we found that the reduction in RC/ABS was the main reason for the reduction in  $PI_{ABS}$  in the Zn treatment in both rice varieties.  $\psi_{E_0}$  and RC/ABS were the main reasons for the reduced  $PI_{ABS}$  for -P, -P-Fe, and -P-Fe-Zn in the CB9 cultivar and the -P-Zn treatment of the BJ1 cultivar. The reduction in  $PI_{ABS}$  values for the remaining treatments was not only influenced by the reduction in  $\psi_{E_0}$  and RC/ABS but also by the reduction in  $\varphi_{P_0}$  values. In particular, the -Fe-Zn treatment exhibited the most pronounced performance, with the lowest overall PSII performance. In addition, the decrease in  $PI_{ABS}$  values for the -P-Fe and -P-Fe-Zn treatments of the CB9 cultivar was lower than that of the -Fe treatment, which we attribute by comparison and analysis to the increased RC/ABS (Table 1). Nam et al. [12] showed that under -P-Fe treatment, plants maintained a green phenotype by regulating the transport of chloroplast ascorbic acid to scavenge reactive oxygen species. This may be the reason why the PSII of CB9 maintained a higher active

reaction center density, promoting an increase in  $\varphi_{P_0}$ , resulting in higher  $PI_{ABS}$  values for the CB9 cultivar under -P-Fe, as well as -P-Fe-Zn, than for -Fe. The BJ1 cultivar did not show a similar trend, probably because of cultivar-specific characteristics.

## 5. Conclusions

In summary, deficiencies of P, Fe, Zn, and their combinations inhibited the growth and photosynthetic characteristics of rice seedlings, and the two varieties showed commonalities and differences. The degree of inhibition of rice seedling growth by the different elements and their combinations was approximately  $-Zn \leq -P-Zn < -P < -P-Fe \leq -P-Fe-Zn \leq -Fe-Zn = -Fe$ , with the BJ1 cultivar showing no significant differences in the -P-Fe, -P-Fe-Zn, -Fe-Zn, and -Fe conditions. In terms of affecting photosynthetic characteristics of the uppermost spreading leaves of seedlings, the reduction in the concentration of active reaction centers under the -Zn treatment was the main reason for the suppression of the overall performance of PSII. The -P treatment reduced the concentration of the active reaction centers and inhibited electron transport. The -P-Zn treatment was more severely disruptive than the -P treatment, and the primary photochemical reaction of the rice seedlings was also inhibited. The -Fe and -Fe-Zn treatments most severely inhibited photosynthesis in seedling leaves, reducing the concentration of active reaction centers and disrupting the energy transfer connectivity of antenna pigments with the PSII active reaction center. This resulted in extremely inefficient energy uptake and transfer from the PSII reaction centers, leaving less electron flux per reaction center to reach and reduce the PSI-terminal electron acceptors. In addition, the maximum carboxylation efficiency  $V_{c,max}$  and the maximum electron transfer rate  $J_{max}$  during carbon assimilation were severely inhibited, severely suppressing the photosynthetic characteristics of seedlings; a similar phenomenon was observed for the -P-Fe and -P-Fe-Zn treatments of the BJ1 cultivar. Unlike the BJ1 cultivar, the -P-Fe and -P-Fe-Zn of the CB9 cultivar increased the density of active unit reaction centers, mitigating the extent of electron transport chain disruption and alleviating the limitation of Fe deficiency, which was probably due to the regulation of -P and -Fe. These data provide insights into the effects of multiple-nutrient deficiencies on the photosynthetic physiology of rice seedlings. It helps to enhance the understanding of the complex relationship between nutrient balance and photosynthesis, especially for P, Fe, Zn, and their combined deficiencies. It also provides some theoretical basis for identifying combined-nutrient deficiencies by rice phenotype and chlorophyll fluorescence.

**Author Contributions:** Formal analysis D.G. and K.D., Writing—Original Draft, D.G., C.R. and K.D.; Writing—Review and Editing, X.W. Conceptualization, Y.Z. Investigation, X.W. Formal analysis, Z.G. Supervision, Y.G. and S.L. Project administration, Resources, Y.G. and L.G. Conceptualization, X.S. Resources, X.S. and L.G. Validation, X.S. and L.G. All authors have read and agreed to the published version of the manuscript.

**Funding:** This study was supported by National key research and development program (2022YFD15-00501), Open Project of the Key Laboratory of Germplasm Innovation and Physiological Ecology of Cold land Grain Crops, Ministry of Education (CXSTOP202202), and the Jilin Province Major Science and Technology Special Project (20230302008NC).

**Data Availability Statement:** The data that support the findings of this study are available on request from the corresponding author.

**Acknowledgments:** We thank the anonymous referees for their comments and suggestions that led to the improvement of this manuscript.

**Conflicts of Interest:** The authors declare no conflict of interest.

## Appendix A

Table A1. Technical fluorescence parameters.

Technical Fluorescence Parameters	
$F_t$	fluorescence at time t after onset of actinic illumination
$F_O = F_{20\mu s}$	minimal fluorescence, when all PSII RCs are open
$F_L = F_{150\mu s}$	fluorescence intensity at the L step (150 $\mu s$ ) of OJIP
$F_K = F_{300\mu s}$	fluorescence intensity at the K step (300 $\mu s$ ) of OJIP
$F_J = F_{2ms}$	fluorescence intensity at the J step (2 ms) of OJIP
$F_I = F_{30ms}$	fluorescence intensity at the I step (30 ms) of OJIP
$F_M (=F_P)$	maximal recorded fluorescence intensity, at the peak P of OJIP
$V_t = (F_t - F_O)/(F_M - F_O)$	relative variable fluorescence at time t
$V_J = (F_J - F_O)/(F_M - F_O)$	relative variable fluorescence at the J step
$W_L = (F_{150\mu s} - F_O)/(F_L - F_O)$	relative variable fluorescence at the L step to the amplitude $F_K - F_O$
$W_K = (F_{300\mu s} - F_O)/(F_J - F_O)$	relative variable fluorescence at the K step to the amplitude $F_J - F_O$
$W_{OJ} = (F_t - F_O)/(F_J - F_O)$	ratio of variable fluorescence $F_t - F_O$ to the amplitude $F_J - F_O$
$W_{OI} = (F_t - F_O)/(F_I - F_O)$	ratio of variable fluorescence $F_t - F_O$ to the amplitude $F_I - F_O$
Quantum efficiencies or flux ratios	
$\varphi_{P_0} = TR_0/ABS = 1 - F_O/F_M$	maximum quantum yield for primary photochemistry
$\psi_{E_0} = ET_0/TR_0 = 1 - V_J$	Efficiency with which a PSII trapped electron is transferred from $Q_A^-$ to PQ
$\varphi_{E_0} = ET_0/ABS = (1 - F_O/F_M)(1 - V_J)$	quantum yield for electron transport (ET)
$\varphi_{D_0} = 1 - \varphi_{P_0} = F_O/F_M$	quantum yield (at t = 0) of energy dissipation
$\varphi_{R_0} = RE_0/ABS = \varphi_{P_0} \bullet \psi_{E_0} \bullet \delta_{R_0} = \varphi_{P_0} \bullet (1 - V_I)$	quantum yield for reduction of the end electron acceptors at the PSI acceptor side (RE)
$\psi_{R_0} = RE_0/TR_0 = \psi_{E_0} \bullet \delta_{R_0} = 1 - V_I$	Efficiency with which a PSII trapped electron is transferred to final PSI acceptors
$\delta_{R_0} = RE_0/ET_0 = (1 - V_I)/(1 - V_J)$	probability that an electron is transported from the reduced intersystem electron acceptors to the final electron acceptors of PSI (RE)
Specific energy fluxes (per $Q_A^-$ reducing PSII reaction centre-RC)	
$ABS/RC = M_0(1/V_J)(1/\varphi_{P_0})$	Absorbed photon flux per active PSII
$TR_0/RC = M_0(1/V_J)$	Trapped energy flux per active PSII
$DI_0/RC = ABS/RC - TR_0/RC$	Dissipated energy (as heat and fluorescence) flux per active PSII
$ET_0/RC = M_0(1/V_J)(1 - V_J)$	Electron flux from $Q_A^-$ to the PQ pool per active PSII
$RE_0/RC = M_0(1/V_J)(1 - V_I)$	Electron flux from $Q_A^-$ to the final electron acceptors of PSI per active PSII
Performance indexes	
$PI_{ABS} = \gamma_{RC}(1 - \gamma_{RC}) \bullet \varphi_{P_0}(1 - \varphi_{P_0}) \bullet \psi_{E_0}(1 - \psi_{E_0})$	performance index (potential) for energy conservation from photons absorbed by PSII to the reduction of intersystem electron acceptors

Subscript "0" (or "O" when written after another subscript) indicates that the parameter refers to the onset of illumination, when all RCs are assumed to be open.

## References

- Tian, S.; Liang, S.; Qiao, K.; Wang, F.; Zhang, Y.; Chai, T. Co-Expression of Multiple Heavy Metal Transporters Changes the Translocation, Accumulation, and Potential Oxidative Stress of Cd and Zn in Rice (*Oryza sativa*). *J. Hazard. Mater.* **2019**, *380*, 120853. [[CrossRef](#)] [[PubMed](#)]
- Hussain, M.; Ahmad, S.; Hussain, S.; Lal, R.; Ul-Allah, S.; Nawaz, A. Rice in Saline Soils: Physiology, Biochemistry, Genetics, and Management. *Adv. Agron.* **2018**, *148*, 231–287. [[CrossRef](#)]
- Mahender, A.; Swamy, B.P.M.; Anandan, A.; Ali, J. Tolerance of Iron-Deficient and -Toxic Soil Conditions in Rice. *Plants* **2019**, *8*, 31. [[CrossRef](#)] [[PubMed](#)]
- Chaiwong, N.; Prom, U.T.C.; Bouain, N.; Lacombe, B.; Rouached, H. Individual Versus Combinatorial Effects of Silicon, Phosphate, and Iron Deficiency on the Growth of Lowland and Upland Rice Varieties. *Int. J. Mol. Sci.* **2018**, *19*, 899. [[CrossRef](#)] [[PubMed](#)]
- Liu, C.; Gao, T.; Liu, Y.; Liu, J.; Li, F.; Chen, Z.; Li, Y.; Lv, Y.; Song, Z.; Reinfelder, J.R.; et al. Isotopic Fingerprints Indicate Distinct Strategies of Fe Uptake in Rice. *Chem. Geol.* **2019**, *524*, 323–328. [[CrossRef](#)]
- Muller, C.; Silveira, S.; Daloso, D.M.; Mendes, G.C.; Merchant, A.; Kuki, K.N.; Oliva, M.A.; Loureiro, M.E.; Almeida, A.M. Ecophysiological Responses to Excess Iron in Lowland and Upland Rice Cultivars. *Chemosphere* **2017**, *189*, 123–133. [[CrossRef](#)]
- Wang, Y.; Zhang, B.; Jiang, D.; Chen, G. Silicon Improves Photosynthetic Performance by Optimizing Thylakoid Membrane Protein Components in Rice Under Drought Stress. *Environ. Exp. Bot.* **2019**, *158*, 117–124. [[CrossRef](#)]
- Li, Y.T.; Xu, W.W.; Ren, B.Z.; Zhao, B.; Zhang, J.; Liu, P.; Zhang, Z.S. High Temperature Reduces Photosynthesis in Maize Leaves by Damaging Chloroplast Ultrastructure and Photosystem II. *J. Agron. Crop Sci.* **2020**, *206*, 548–564. [[CrossRef](#)]

9. Mongon, J.; Chaiwong, N.; Bouain, N.; Prom, U.T.C.; Secco, D.; Rouached, H. Phosphorus and Iron Deficiencies Influences Rice Shoot Growth in an Oxygen Dependent Manner: Insight from Upland and Lowland Rice. *Int. J. Mol. Sci.* **2017**, *18*, 607. [[CrossRef](#)]
10. Kalaji, H.M.; Jajoo, A.; Oukarroum, A.; Brestic, M.; Zivcak, M.; Samborska, I.A.; Cetner, M.D.; Łukasik, I.; Goltsev, V.; Ladle, R.J. Chlorophyll a Fluorescence as a Tool to Monitor Physiological Status of Plants under Abiotic Stress Conditions. *Acta Physiol. Plant.* **2016**, *38*, 102. [[CrossRef](#)]
11. Ding, Y.; Wang, Z.; Ren, M.; Zhang, P.; Li, Z.; Chen, S.; Ge, C.; Wang, Y. Iron and Callose Homeostatic Regulation in Rice Roots under Low Phosphorus. *BMC Plant Biol.* **2018**, *18*, 326. [[CrossRef](#)] [[PubMed](#)]
12. Nam, H.I.; Shahzad, Z.; Dorone, Y.; Clowez, S.; Zhao, K.; Bouain, N.; Lay-Pruitt, K.S.; Cho, H.; Rhee, S.Y.; Rouached, H. Interdependent Iron and Phosphorus Availability Controls Photosynthesis through Retrograde Signaling. *Nat. Commun.* **2021**, *12*, 7211. [[CrossRef](#)] [[PubMed](#)]
13. Yadavalli, V.; Neelam, S.; Rao, A.S.; Reddy, A.R.; Subramanyam, R. Differential Degradation of Photosystem I Subunits under Iron Deficiency in Rice. *J. Plant Physiol.* **2012**, *169*, 753–759. [[CrossRef](#)] [[PubMed](#)]
14. Msilini, N.; Essemine, J.; Zaghdoudi, M.; Harnois, J.; Lachaal, M.; Ouergui, Z.; Carpentier, R. How Does Iron Deficiency Disrupt the Electron Flow in Photosystem I of Lettuce Leaves? *J. Plant Physiol.* **2013**, *170*, 1400–1406. [[CrossRef](#)]
15. Therby-Vale, R.; Lacombe, B.; Rhee, S.Y.; Nussaume, L.; Rouached, H. Mineral Nutrient Signaling Controls Photosynthesis: Focus on Iron Deficiency-Induced Chlorosis. *Trends Plant Sci.* **2022**, *27*, 502–509. [[CrossRef](#)]
16. Plant Nutrition 3: Micronutrients and metals. *Plant Cell* **2015**, *27*. [[CrossRef](#)]
17. Ji, C.; Li, J.; Jiang, C.; Zhang, L.; Shi, L.; Xu, F.; Cai, H. Zinc and Nitrogen Synergistic Act on Root-to-Shoot Translocation and Preferential Distribution in Rice. *J. Adv. Res.* **2022**, *35*, 187–198. [[CrossRef](#)]
18. Zhang, J.; Wang, S.; Song, S.; Xu, F.; Pan, Y.; Wang, H. Transcriptomic and Proteomic Analyses Reveal New Insight into Chlorophyll Synthesis and Chloroplast Structure of Maize Leaves under Zinc Deficiency Stress. *J. Proteom.* **2019**, *199*, 123–134. [[CrossRef](#)]
19. Bouain, N.; Krouk, G.; Lacombe, B.; Rouached, H. Getting to the Root of Plant Mineral Nutrition: Combinatorial Nutrient Stresses Reveal Emergent Properties. *Trends Plant Sci.* **2019**, *24*, 542–552. [[CrossRef](#)]
20. Hanikenne, M.; Esteves, S.M.; Fanara, S.; Rouached, H. Coordinated Homeostasis of Essential Mineral Nutrients: A Focus on Iron. *J. Exp. Bot.* **2021**, *72*, 2136–2153. [[CrossRef](#)]
21. Medici, A.; Szponarski, W.; Dangeville, P.; Safi, A.; Dissanayake, I.M.; Saenchai, C.; Emanuel, A.; Rubio, V.; Lacombe, B.; Ruffel, S.; et al. Identification of Molecular Integrators Shows that Nitrogen Actively Controls the Phosphate Starvation Response in Plants. *Plant Cell.* **2019**, *31*, 1171–1184. [[CrossRef](#)] [[PubMed](#)]
22. Ding, Y.; Wang, Z.; Mo, S.; Liu, J.; Xing, Y.; Wang, Y.; Ge, C.; Wang, Y. Mechanism of Low Phosphorus Inducing the Main Root Lengthening of Rice. *J. Plant Growth Regul.* **2020**, *40*, 1032–1043. [[CrossRef](#)]
23. Khaliq, M.A.; James, B.; Chen, Y.H.; Ahmed Saqib, H.S.; Li, H.H.; Jayasuriya, P.; Guo, W. Uptake, Translocation, and Accumulation of Cd and Its Interaction with Mineral Nutrients (Fe, Zn, Ni, Ca, Mg) in Upland Rice. *Chemosphere* **2019**, *215*, 916–924. [[CrossRef](#)] [[PubMed](#)]
24. Niyigaba, E.; Twizerimana, A.; Mugenzi, I.; Ngnadong, W.A.; Ye, Y.P.; Wu, B.M.; Hai, J.B. Winter Wheat Grain Quality, Zinc and Iron Concentration Affected by a Combined Foliar Spray of Zinc and Iron Fertilizers. *Agronomy* **2019**, *9*, 250. [[CrossRef](#)]
25. Yoshida, S.; Forno, D.A.; Cock, J.H. *Laboratory Manual for Physiological Studies of Rice*; The International Rice Research Institute: Los Baños, Philippines, 1976.
26. Stinziano, J.R.; Morgan, P.B.; Lynch, D.J.; Saathoff, A.J.; McDermit, D.K.; Hanson, D.T. The Rapid A-Ci Response: Photosynthesis in the Phenomic Era. *Plant Cell Environ.* **2017**, *40*, 1256–1262. [[CrossRef](#)] [[PubMed](#)]
27. Farquhar, G.D.; von Caemmerer, S.; Berry, J.A. A Biochemical Model of Photosynthetic CO<sub>2</sub> Assimilation in Leaves of C<sub>3</sub> Species. *Planta* **1980**, *149*, 78–90. [[CrossRef](#)] [[PubMed](#)]
28. Strasser, R.J.; Tsimilli-Michael, M.; Srivastava, A. Analysis of the Chlorophyll a Fluorescence Transient. In *Chlorophyll a Fluorescence; Advances in Photosynthesis and Respiration*; Papageorgiou, G.C., Govindjee, J., Eds.; Springer: Dordrecht, The Netherlands, 2004; Volume 19. [[CrossRef](#)]
29. Strasser, R.J.; Tsimilli-Michael, M.; Dangre, D.; Rai, M. Biophysical Phenomics Reveals Functional Building Blocks of Plants Systems Biology: A Case Study for the Evaluation of the Impact of Mycorrhization with *Piriformospora indica*. In *Advanced Techniques in Soil Microbiology; Soil Biology*; Varma, A., Oelmüller, R., Eds.; Springer: Berlin/Heidelberg, Germany, 2007; Volume 11. [[CrossRef](#)]
30. Guo, Y.; Lu, Y.; Goltsev, V.; Strasser, R.J.; Kalaji, H.M.; Wang, H.; Wang, X.; Chen, S.; Qiang, S. Comparative Effect of Tenuazonic Acid, Diuron, Bentazone, Dibromothymoquinone and Methyl Viologen on the Kinetics of Chl a Fluorescence Rise OJIP and the MR820 Signal. *Plant Physiol. Biochem.* **2020**, *156*, 39–48. [[CrossRef](#)]
31. Strasser, R.J.; Tsimilli-Michael, M.; Qiang, S.; Goltsev, V. Simultaneous in vivo Recording of Prompt and Delayed Fluorescence and 820-nm Reflection Changes During Drying and after Rehydration of the Resurrection Plant *Haberlea Rhodopensis*. *Biochim. Biophys. Acta* **2010**, *1797*, 1313–1326. [[CrossRef](#)]
32. Kalaji, H.M.; Schansker, G.; Ladle, R.J.; Goltsev, V.; Bosa, K.; Allakhverdiev, S.I.; Brestic, M.; Bussotti, F.; Calatayud, A.; Dabrowski, P.; et al. Frequently Asked Questions about in vivo Chlorophyll Fluorescence: Practical Issues. *Photosynth. Res.* **2014**, *122*, 121–158. [[CrossRef](#)]

33. Kalaji, H.M.; Oukarroum, A.; Alexandrov, V.; Kouzmanova, M.; Brestic, M.; Zivcak, M.; Samborska, I.A.; Cetner, M.D.; Al-lakhverdiev, S.I.; Goltsev, V. Identification of Nutrient Deficiency in Maize and Tomato Plants by in Vivo Chlorophyll a Fluorescence Measurements. *Plant Physiol. Biochem.* **2014**, *81*, 16–25. [[CrossRef](#)]
34. Kalaji, H.M.; Baba, W.; Gediga, K.; Goltsev, V.; Samborska, I.A.; Cetner, M.D.; Dimitrova, S.; Piszcz, U.; Bielecki, K.; Karmowska, K.; et al. Chlorophyll Fluorescence as a Tool for Nutrient Status Identification in Rapeseed Plants. *Photosynth. Res.* **2018**, *136*, 329–343. [[CrossRef](#)] [[PubMed](#)]
35. Saenchai, C.; Bouain, N.; Kisko, M.; Prom, U.T.C.; Dumas, P.; Rouached, H. The Involvement of OsPHO1;1 in the Regulation of Iron Transport Through Integration of Phosphate and Zinc Deficiency Signaling. *Front. Plant Sci.* **2016**, *7*, 396. [[CrossRef](#)] [[PubMed](#)]
36. Szerement, J.; Szatanik-Kloc, A.; Mokrzycki, J.; Mierzwa-Hersztek, M. Agronomic Biofortification with Se, Zn, and Fe: An Effective Strategy to Enhance Crop Nutritional Quality and Stress Defense—A Review. *J. Soil Sci. Plant Nut.* **2021**, *22*, 1129–1159. [[CrossRef](#)]
37. Shen, J.; Li, X.; Zhu, X.; Ding, Z.; Huang, X.; Chen, X.; Jin, S. Molecular and Photosynthetic Performance in the Yellow Leaf Mutant of *Torreyia grandis* According to Transcriptome Sequencing, Chlorophyll a Fluorescence, and Modulated 820 nm Reflection. *Cells* **2022**, *11*, 431. [[CrossRef](#)]
38. Bano, H.; Athar, H.U.; Zafar, Z.U.; Kalaji, H.M.; Ashraf, M. Linking changes in chlorophyll a fluorescence with drought stress susceptibility in mung bean [*Vigna radiata* (L.) Wilczek]. *Physiol. Plant.* **2021**, *172*, 1244–1254. [[CrossRef](#)] [[PubMed](#)]
39. Yoneyama, T.; Ishikawa, S.; Fujimaki, S. Route and Regulation of Zinc, Cadmium, and Iron Transport in Rice Plants (*Oryza sativa* L.) during Vegetative Growth and Grain Filling: Metal Transporters, Metal Speciation, Grain Cd Reduction and Zn and Fe Biofortification. *Int. J. Mol. Sci.* **2015**, *16*, 19111–19129. [[CrossRef](#)] [[PubMed](#)]
40. Paunov, M.; Koleva, L.; Vassilev, A.; Vangronsveld, J.; Goltsev, V. Effects of Different Metals on Photosynthesis: Cadmium and Zinc Affect Chlorophyll Fluorescence in Durum Wheat. *Int. J. Mol. Sci.* **2018**, *19*, 787. [[CrossRef](#)]
41. Adil, M.F.; Sehar, S.; Han, Z.; Wa Lwalaba, J.L.; Jilani, G.; Zeng, F.; Chen, Z.H.; Shamsi, I.H. Zinc Alleviates Cadmium Toxicity by Modulating Photosynthesis, ROS Homeostasis, and Cation Flux Kinetics in Rice. *Environ. Pollut.* **2020**, *265 Pt B*, 114979. [[CrossRef](#)]
42. Chen, S.; Strasser, R.J.; Qiang, S. In vivo assessment of effect of phytotoxin tenuazonic acid on PSII reaction centers. *Plant Physiol. Biochem.* **2014**, *84*, 10–21. [[CrossRef](#)]

**Disclaimer/Publisher’s Note:** The statements, opinions and data contained in all publications are solely those of the individual author(s) and contributor(s) and not of MDPI and/or the editor(s). MDPI and/or the editor(s) disclaim responsibility for any injury to people or property resulting from any ideas, methods, instructions or products referred to in the content.